https://ntrs.nasa.gov/search.jsp?R=19690004942 2018-07-23T14:05:17+00:00Z

N 69 14276
NASA CR 98654

CASE FILE COPY

RIGIDITY PROPERTIES OF A THREE-WAY PRESTRESSED SEGMENTED CERAMIC PLATE

September 1968

Report No. 68-57

C.P. Chen
R.B. Matthiesen

Report No. 68-57
September 1968

RIGIDITY PROPERTIES OF A THREE-WAY PRESTRESSED SEGMENTED CERAMIC PLATE

C. P. Chen
R. B. Matthiesen

DEPARTMENT OF ENGINEERING
UNIVERSITY OF CALIFORNIA
LOS ANGELES, CALIFORNIA

published by
Department of Engineering
Reports Group
University of California
Los Angeles, California 90024

ACKNOWLEDGMENTS

The research described in this report was supported by the National Aeronautics and Space Administration under Grants NsG-423 and NsG-427. The authors also wish to thank Professors F.R. Shanley and W.J. Knapp for their helpful advice and encouragement.

TABLE OF CONTENTS

	Page
LIST OF FIGURES	vii
ABSTRACT	ix
I. INTRODUCTION	1
II. DESCRIPTION OF THE PRESTRESSED SEGMENTED PLATE	7
III. EXPERIMENTAL PROGRAM AND RESULTS	13
IV. SUMMARY AND CONCLUSIONS	41
BIBLIOGRAPHY	43
APPENDIX	45

LIST OF FIGURES

Figure		Page
1	Three-Way Prestressed Ceramic Plate	2
2	Overall Dimensions of the Test Plate	3
3	Arrangement of the Steel Rods and End Anchorage System	8
4	Full Size Ceramic Segment	9
5	Prestressing Fixture	11
6	Test for D_{x_1} and D_{y_1} Cylindrical Bending in x_1-Axis and y_1-Axis	14
7	Test for D_{x_2} and D_{y_2} Cylindrical Bending in x_2-Axis and y_2-Axis	15
8	Test for D_{x_3} and D_{y_3} Cylindrical Bending in x_3-Axis and y_3-Axis	16
9	Cylindrical Bending Test	17
10	Moment Versus Curvature for Cylindrical Bending in x_1-Axis	20
11	Moment Versus Curvature for Cylindrical Bending in x_2-Axis	21
12	Moment Versus Curvature for Cylindrical Bending in x_3-Axis	22
13	Moment Versus Curvature for Cylindrical Bending in y_1-Axis	23
14	Moment Versus Curvature for Cylindrical Bending in y_2-Axis	24
15	Moment Versus Curvature for Cylindrical Bending in y_3-Axis	25
16	Twisting Test, Front View	27
17	Layout of Three Squares (35-3/8" x 35-3/8" on the Slab for Twisting Tests	29
18	Force Versus Deflection of Twisting Test for $D_{x_1y_1}$	30
19	Force Versus Deflection of Twisting Test for $D_{x_2y_2}$	31
20	Force Versus Deflection of Twisting Test for $D_{x_3y_3}$	32
21	Anticlastic Bending Test	35
22	Moment Versus Curvature for Anticlastic Bending in y_1-Direction Direction	37
23	Moment Versus Curvature for Anticalstic Bending in y_2-Direction	38

LIST OF FIGURES (Continued)

Figure		Page
24	Moment Versus Curvature for Anticlastic Bending in y_3-Direction	39
A1	Curvature Gage and Bent Plate	46
A2	Plate Under Twisting Moment	48

ABSTRACT

Experimental methods used in an investigation of a three-way prestressed ceramic plate comprised of triangular segments are discussed. The rigidity properties of interest were the bending, twisting and Poisson rigidity constants D_{x_i}, D_{y_i}, $D_{x_i y_i}$ and D_{I_i} in three coplanar directions with an angle of 120 degrees from one to another.

The experimentation involved two cylindrical bending tests to determine the flexural rigidities D_{x_i} and D_{y_i}, a twisting test to obtain the twisting rigidity $D_{x_i y_i}$, and an anticlastic bending test to examine the Poisson's rigidity D_{I_i}.

The results of experiments on the hexagonal ceramic plate prestressed in three directions are presented and compared with the ordinary theory of orthotropic plates. The results indicate that the plate has three sets of "principal" axes in the plane.

I INTRODUCTION

As a part of a continuing research program in structural applications of ceramics,[1, 2, 3] the bending stiffness properties of a three-way prestressed ceramic plate comprised of triangular segments were determined experimentally. The intent of this study was to provide information which would be useful in the design of prestressed segmented plates. Subsequently, the research program will include studies of prestressed segmented domes. While it was felt that the membrane characteristics of such domes may be readily determined directly from the test of these domes, the bending characteristics are not as readily obtained. Thus, the bending tests of the segmented plate also are useful in indicating the nature of the bending properties which are to be expected to exist in prestressed segmented domes.

Ideally, the experimentally-determined behavior of the segmented plate should be compared to some appropriate theory of behavior for such a plate. In a previous study of a prestressed segmented plate with square segments,[2] it was found that the behavior could be represented in terms of orthotropic plate theory.[4, 5, 6, 7, 8] The present investigation indicates that orthotropic plate theory is not adequate for representing the behavior of the plate with triangular elements and prestressing in three directions. However, orthotropic plate theory is the best guide which could be found for planning the tests.

The prestressed plate used in this investigation is shown in Figure 1. As indicated later, the behavior of the plate is anisotropic with three sets of orthotropic axes in the plane of the plate. This results in three independent sets of "principal" axes in the plane. For discussion purposes, the sets of axes are labeled x_1, y_1; x_2, y_2; x_3, y_3 as shown in Figure 2. The overall dimensions of the plate are also shown in Figure 2.

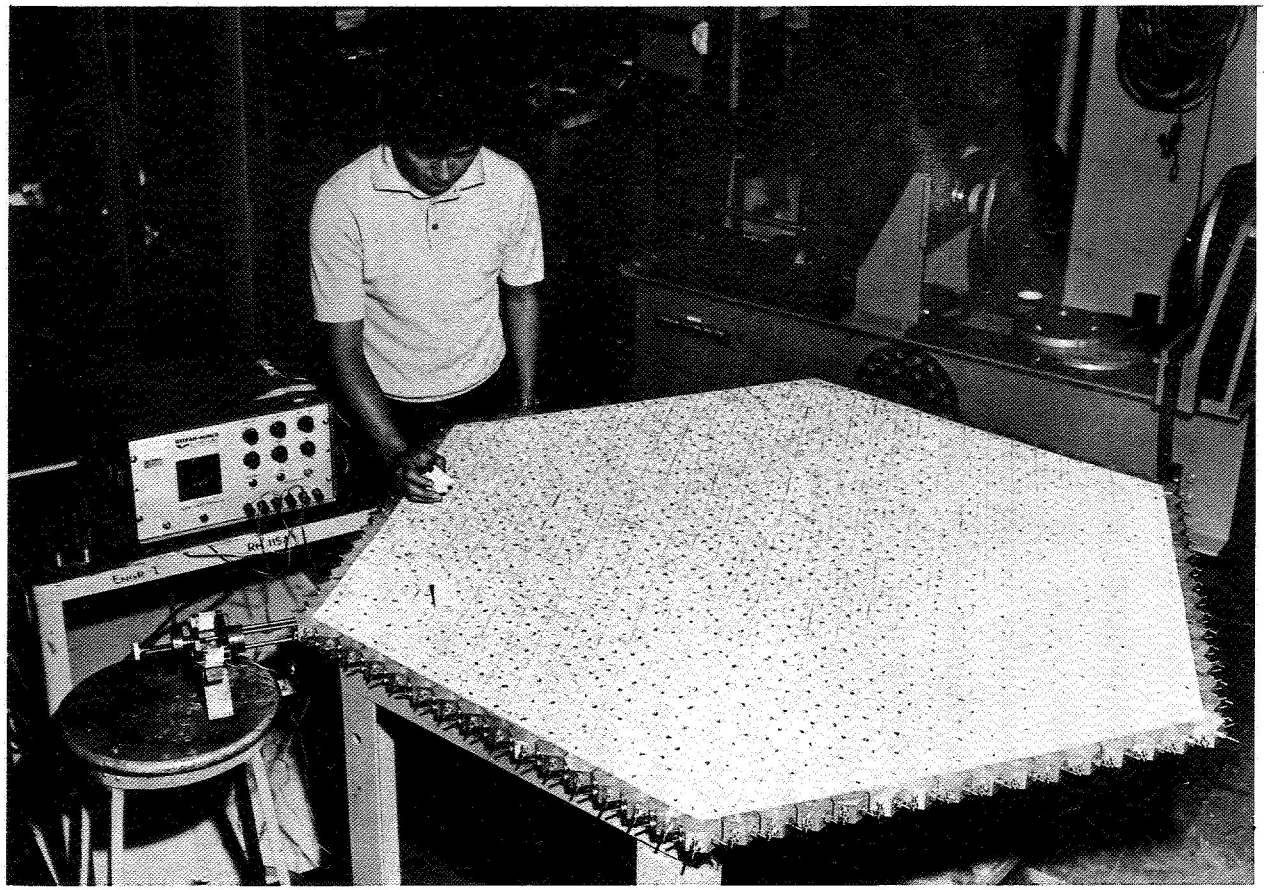

THREE-WAY PRESTRESSED CERAMIC PLATE

Figure 1

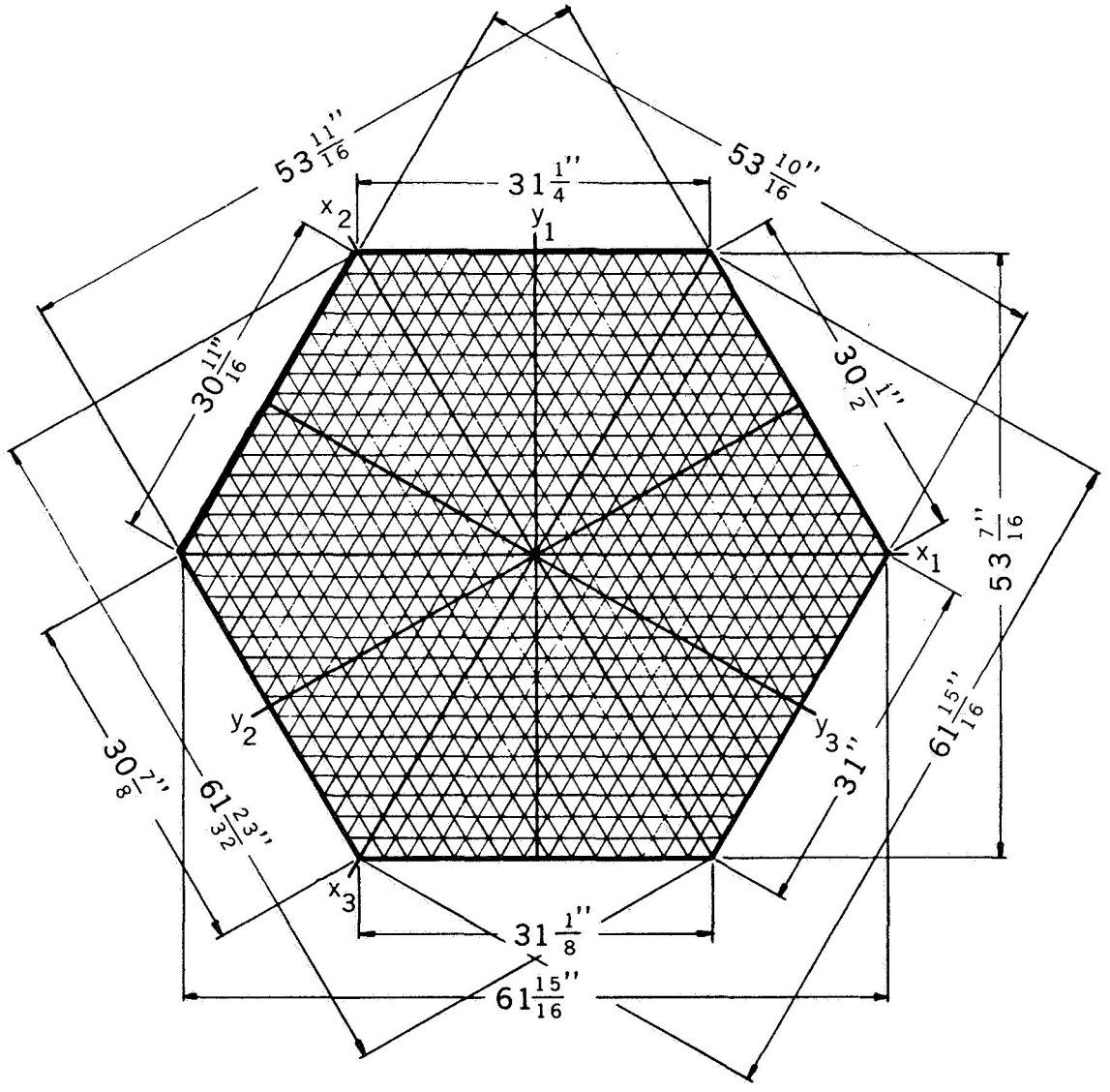

OVERALL DIMENSIONS OF THE TEST PLATE

Figure 2

The governing differential equation for small displacements of an orthotropic plate is given as (5)

$$D_x \frac{\partial^4 w}{\partial x^4} + 2\left(D_I + 2D_{xy}\right) \frac{\partial^4 w}{\partial x^2 \partial y^2} + D_y \frac{\partial^4 w}{\partial y^4} = q*xy)$$

where D_x and D_y are flexural rigidities, D_{xy} is the twisting rigidity, D_I is the Poisson rigidity, and x, y denote a set of orthogonal principal axes.

The rigidity constants are considered to be fundamental properties of an orthotropic plate. Analytically, the relationships between the moments, the curvatures, and the twist of an infinitesimal plate element can be expressed as follows

$$M_x = - D_x \frac{\partial^2 w}{\partial y^2} - D_I \frac{\partial^2 w}{\partial y^2} \tag{1}$$

$$M_y = - D_y \frac{\partial^2 w}{\partial y^2} - D_I \frac{\partial^2 w}{\partial x^2} \tag{2}$$

$$M_{xy} = - 2D_{xy} \frac{\partial^2 w}{\partial x \partial y} \tag{3}$$

where

$$\frac{\partial^2 w}{\partial x^2} = - \frac{1}{R_x} \tag{4}$$

$$\frac{\partial^2 w}{\partial y^2} = - \frac{1}{R_y} \tag{5}$$

$$\frac{\partial^2 w}{\partial x \partial y} = - \frac{1}{R_{xy}} \tag{6}$$

and

w = displacement function, in z-direction

$$\frac{1}{R_x}, \frac{1}{R_y}, \frac{1}{R_{xy}} = \text{radii of curvature}$$

$$M_x, M_y, M_x = \text{moments acting on the plate}$$

Now, if the plate is deformed into a cylindrical surface in the x direction, $\left(\text{i.e.}, \frac{1}{R_y} = 0\right)$ Equations (1) and (5) yield

$$M_x = - D_x \frac{1}{R_x}$$

or

$$D_x = \frac{M_x}{1/R_x} \quad (\text{lb - in}^2/\text{in}) \tag{7}$$

Similarly, if $1/R_x = 0$, Equations (3) and (6) yield

$$D_y = \frac{M_y}{1/R_y} \quad (\text{lb - in}^2/\text{in}) \tag{8}$$

A pure twist may be imposed on the plate by applying four equal vertical forces at the corners of the plate, two diagonally opposite forces acting upwards while the other two act downwards. From Equations (3) and Equation (6), the twisting rigidity is expressed as

$$D_{xy} = \frac{M_{xy}}{2(1/R_{xy})} \quad (\text{lb - in}^2/\text{in}) \tag{9}$$

The plate may be deformed in anticlastic bending, by applying a moment M_y while the plate is permitted to bend about the y-axis. The moment M_y produces a primary curvature $1/R_y$ and a secondary curvature $1/R_x$ due to the Poisson effect. Equation (1) yields:

$$D_I = - D_x \frac{1/R_x}{1/R_y} = D_x \nu_i \tag{10}$$

when

$$M_x = 0$$

Also, from Equation (2)

$$D_i = \frac{1}{1/R_x} \left(M_y - D_y \frac{1}{R_y} \right)$$

if $1/R_x$ (curvature in x direction) is small, this is a less accurate measure of D_I than in Equation (10).

II DESCRIPTION OF THE PRESTRESSED SEGMENTED PLATE

The test plate was a hexagon, which was comprised of 1350 separate equilateral triangular ceramic blocks. The overall dimensions of the plate, shown in Figure 2, were approximately 31 inches on each side and 1-1/4 inches in thickness.

The segments were held together by type 304 stainless steel rods. In order to eliminate the initial bending of the ceramic blocks due to an eccentric prestress, a 3/16-inch diameter rod was used in the x_1-direction through the horizontal center line of the plate and two 1/8-inch diameter rods were employed in each of the x_2 and x_3 directions to maintain the center of gravity of the prestressing steel in each direction at the center line of the block. The detail of this arrangement of the steel rods is shown as Figure 3. The steel rods had an allowable tensile strength of 95,000 psi. The ends of the rod had been threaded and extra thick nuts were used to take the tensile prestress.

All bearing surfaces of the ceramic blocks were protected by rubber impregnated asbestos sheets (Garlock 900, 1/16-inch thick) for better distribution of the load between segments. A half hexagon aluminum end block was placed at each joint on all the edges of the ceramic plate to anchor the tensioning rods and to distribute the load to the ceramic. The total weight of the test plate was 290 pounds.

Each element of the test plate was an equilateral triangular ceramic segment 2 inches in edge length and 1 1/4 inches thick, with a 3/4" x 1/8" groove on the horizontal center line of each side. Figure 4 shows the dimensions of the segment. Slip-casting was used for forming the alumina-feldspar-clay body.[9] The slip contained solids comprised of 50%

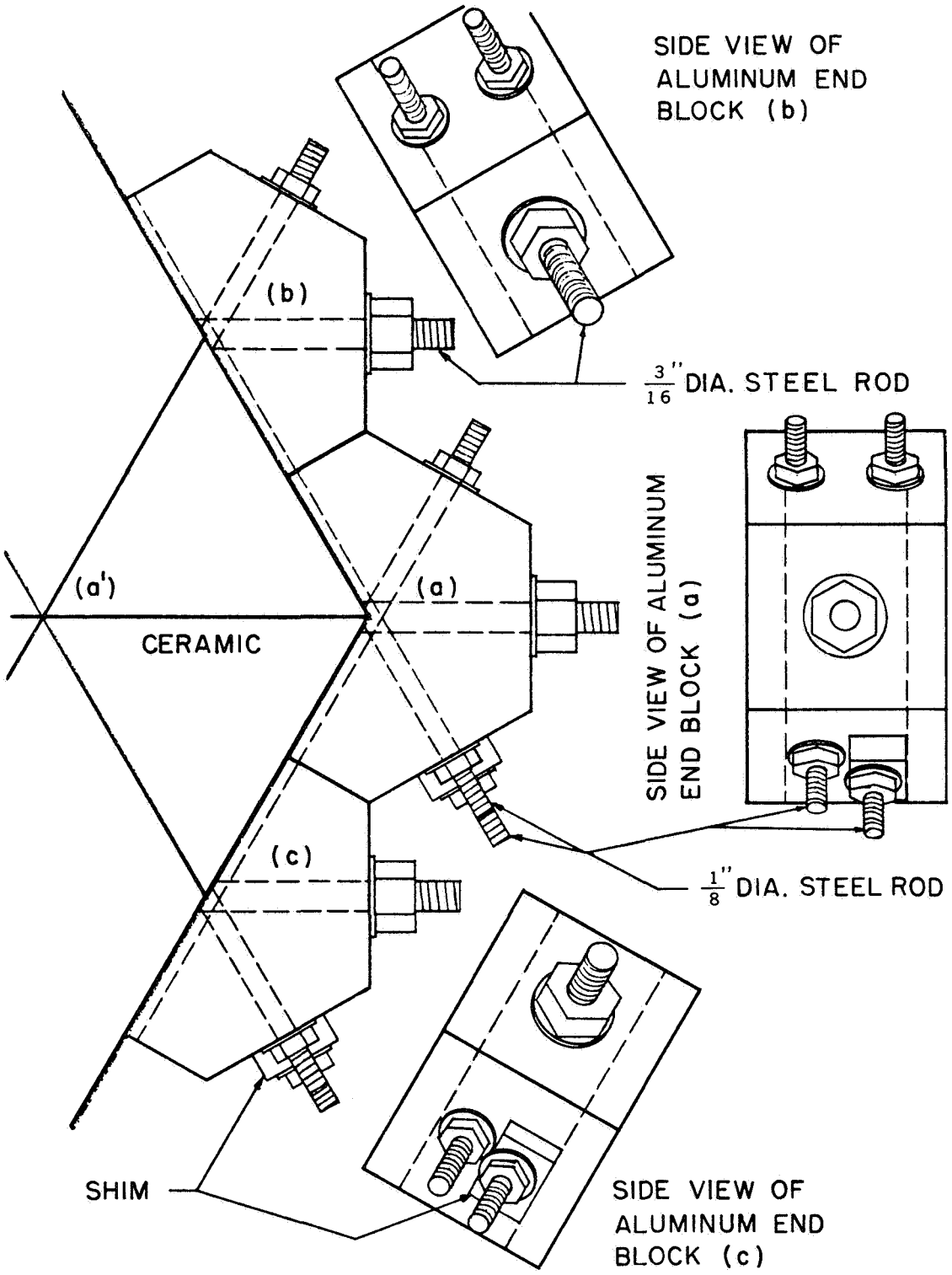

ARRANGEMENT OF THE STEEL RODS AND END ANCHORAGE SYSTEM

Figure 3

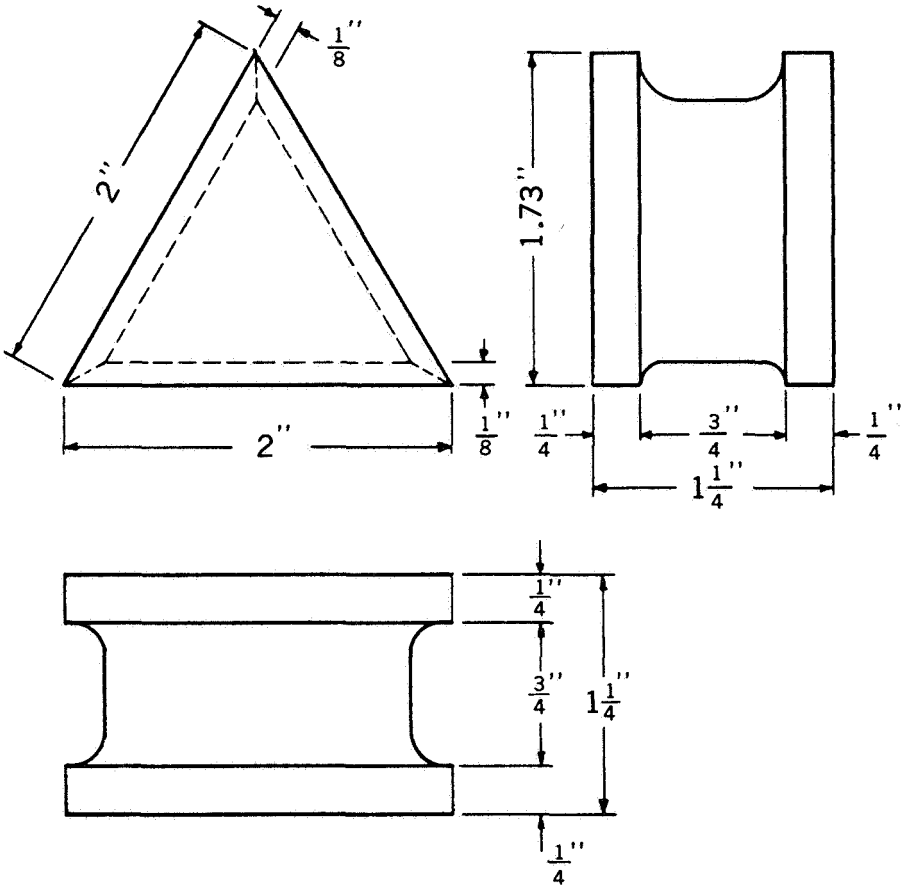

FULL SIZE CERAMIC SEGMENT

Figure 4

aluminum oxide,* 20% feldspar,** and 30% clays† and was deflocculated with sodium silicate. Gypsum plaster molds were used, each mold containing four single triangular segment cavities. The segments were fired in lots by four separate firings. They were fired in an electric kiln at a heating rate of 75°C/hour and held at a 1250°C end-point temperature for 49 hours.

The mechanical properties of the ceramic material were determined to be:

TABLE I

Density.	= 0.0964 lb/in^3 (By A. S. T. M., C 20-46)
Apparent Porosity	= 7.807% (By A. S. T. M., C 20-46)
Absorption (water)	= 2.916% (By A. S. T. M., C 20-46)
Modulus of Elasticity	= 1.5 x 10^7 psi (By A. S. T. M., E 6-62 Sec 11)
Ultimate Compressive Strength.	= 80,000 psi (By A. S. T. M., E 6-62 Sec 5)
Poisson's Ratio.	= 0.20 (By A. S. T. M., E 6-62 Sec 11)

The rod prestress was adjusted individually with the prestressing fixture shown in Figure 5. Two strain gages (Type EA-06-125AS-120) were mounted onto the 5/16" x 1" x 5" cold rolled steel beam at the back of the fixture which had been calibrated as the beam was bent by tightening

* Alcoa T-61 Alumina (-325 mesh tabular), Alumina Company of America, Bauxite, Ark.

** Kingman Feldspar, Consolidated Feldspar Corp., Kona, N.C.

† ASP 900 Kaolin (15%) Minerals and Chemicals, Philipp Corp., Menlo Park, N.J.
Bandy Black Ball Clay (5%), Spinks Clay Co., Paris, Tenn.
Champion and Challenger Ball Clay (10%) Spinks Clay Co., Paris, Tenn.

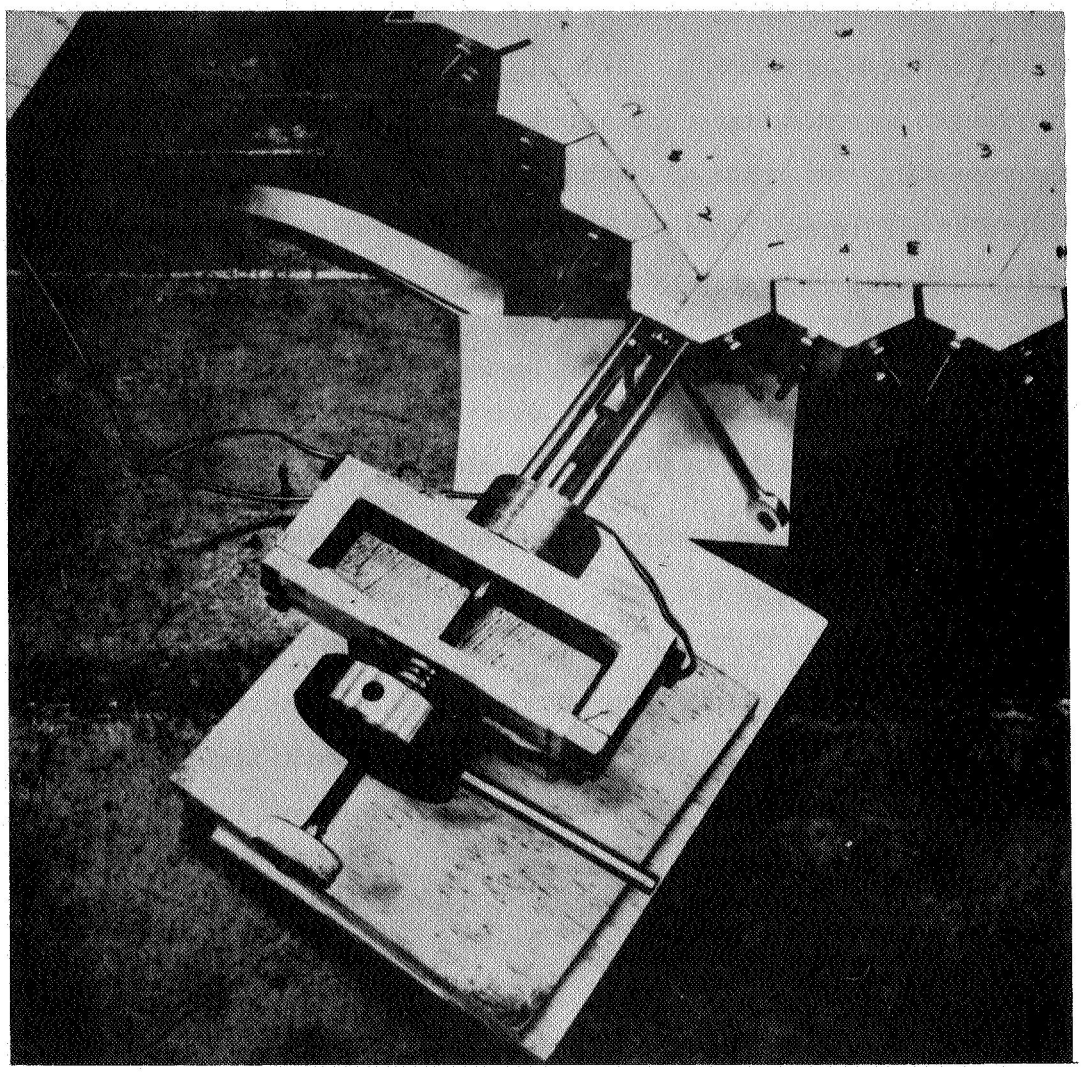

PRESTRESSING FIXTURE

Figure 5

of the screw spindle. There were three sets of legs to fit the three sets of prestressing rods. During prestressing, an adapter from the fixture screwed into the threaded end of the rod to apply the tension, while the legs were reacting against the slab. The anchor nut was turned tight to bring the strain reading back to zero after the rod was stretched to a desired level of prestress. The final level of prestress was achieved in increments by attaining a low level of prestress in each of the rods and then repeating the process so that a nearly uniform state of prestress existed at all times. The prestressing was checked frequently to eliminate the loss of prestress due to tendon extension, creep and shrinkage of the gaskets, etc.

All the experiments were designed to study the rigidity properties under the case of uniform prestress, in the ceramic.

The initial tension applied on each 1/8-inch diameter rod was 400 lb and on each 3/16-inch diameter rod was 800 lb. The tensile prestress in the small rods was 58,000 psi and in the big rods was 42,000 psi at the root of the threaded ends. The maximum compressive stress on the ceramic was about 1,850 psi. The ultimate tensile strength of the stainless steel rod was 100,000 psi and the ultimate compressive strength of the ceramic material was 80,000 psi.

III EXPERIMENTAL PROGRAM AND RESULTS

(a) Cylindrical Bending Tests:

In this test the plate was supported by and loaded through relatively rigid round parallel bars. This caused curvature about one axis and theoretically allowed no curvature about the orthogonal axis. For this case, Equations (7) and (8) may be expressed as

$$D_{x_i} = \frac{M_{x_i}}{1/R_{x_i}}$$

and

$$D_{y_i} = -\frac{M_{x_i}}{1/R_{y_i}}$$

The rigidity constants D_{x_i} and D_{y_i} were obtained by bending the plate about all six axes (x_1, x_2, x_3 and y_1, y_2, y_3) individually. Figures 6, 7 and 8 indicate the location of the load line and support line and the location of the curvature measurements reported herein for each of the cylindrical bending tests. In each case, two tests were made at each of the five points on the plate to measure the x_i and y_i curvatures.

Figure 9 is a photograph of a cylindrical bending test. The force to bend the plate was provided by a two-ton hydraulic jack (Enerpac, RC-120). The plate curvatures were measured by a curvature gage which consisted of a dial gage, reading directly to 10^{-4} inches, mounted at the mid-point of a steel bar with two stationary legs. A description of this instrument is given in Appendix I.

For the conditions of the experiment, (see Figure 6) the average bending moments M_{x_1} and M_{y_1} are:

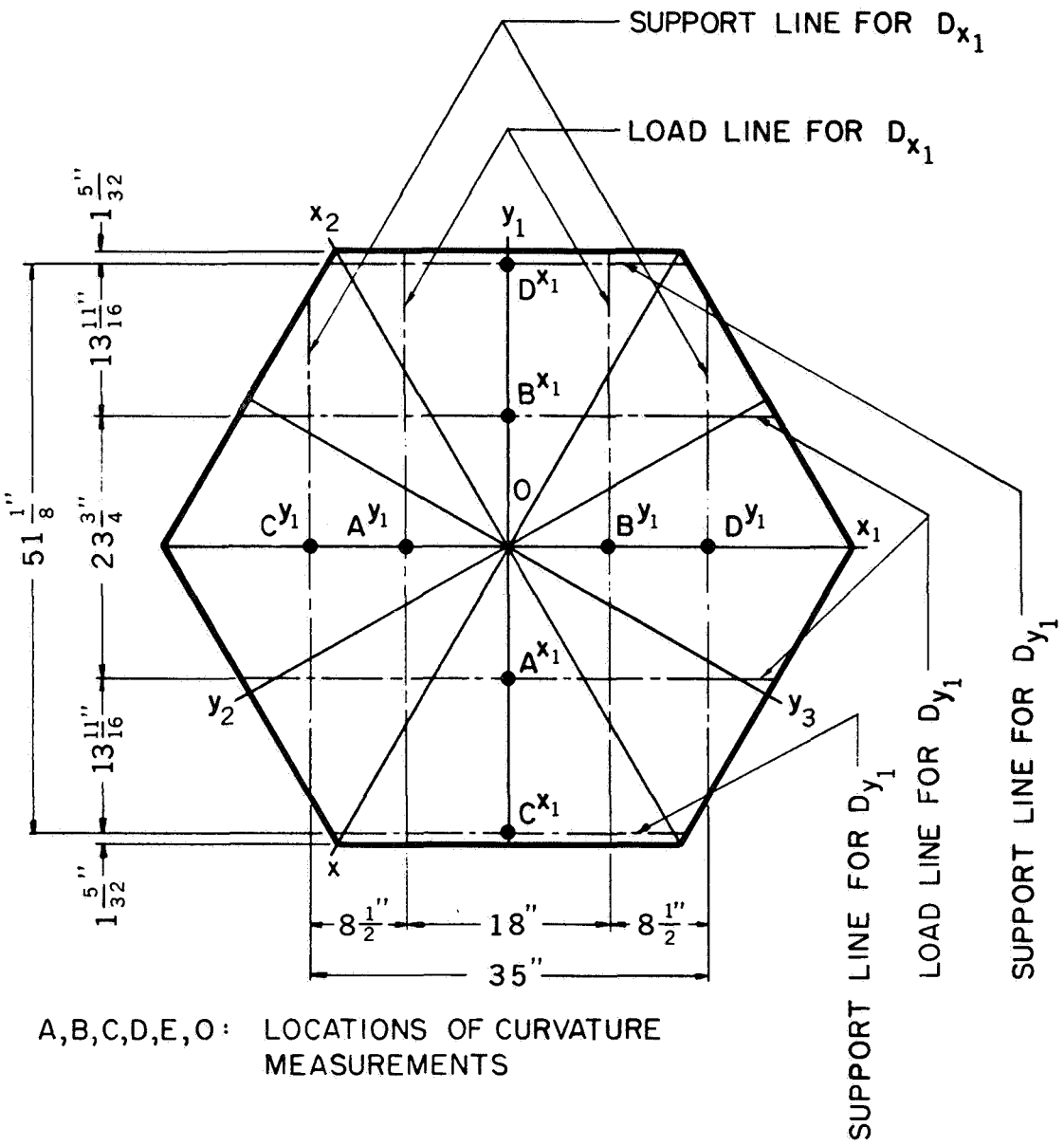

A,B,C,D,E,O: LOCATIONS OF CURVATURE MEASUREMENTS

TEST FOR D_{x_1} AND D_{y_1}

CYLINDRICAL BENDING IN x_1–AXIS AND y_1–AXIS

Figure 6

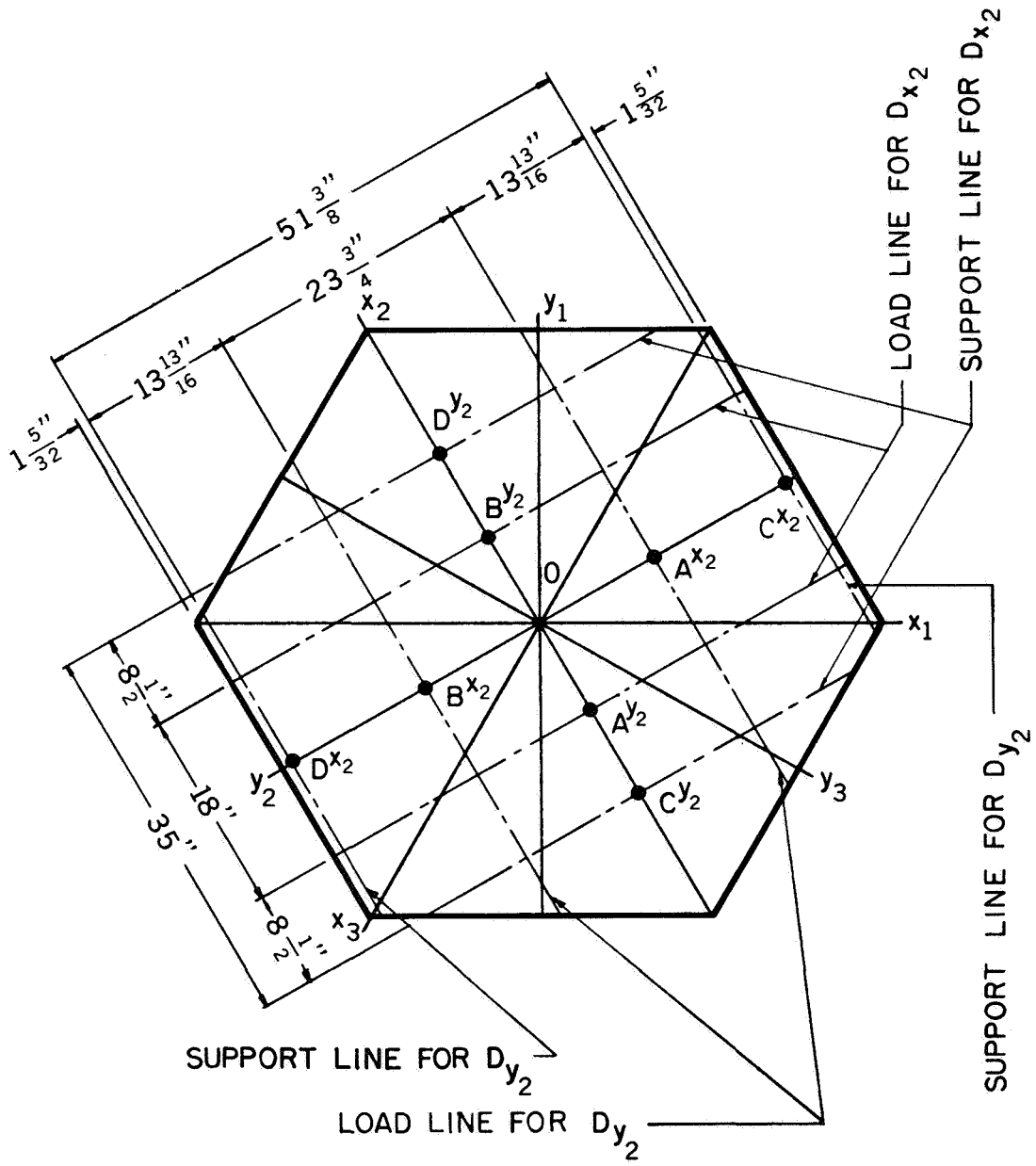

A,B,C,D,O: LOCATIONS OF CURVTURE MEASUREMENTS

TEST FOR D_{x_2} AND D_{y_2}

CYLINDRICAL BENDING IN x_2–AXIS AND y_2–AXIS

Figure 7

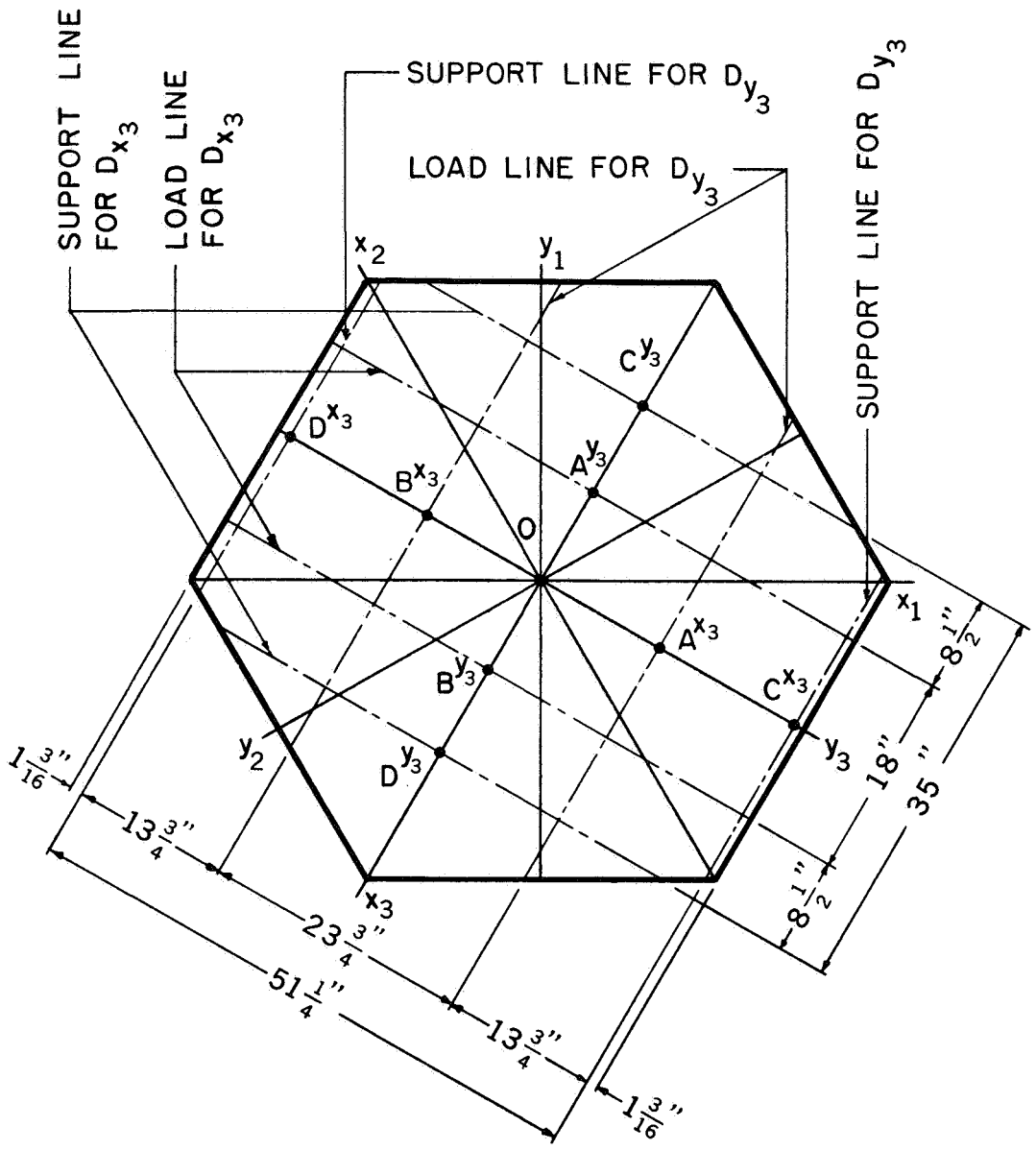

A,B,C,D,O : LOCATIONS OF CURVATURE MEASUREMENTS

TEST FOR D_{x_3} AND D_{y_3}

CYLINDRICAL BENDING IN x_3–AXIS AND y_3–AXIS

Figure 8

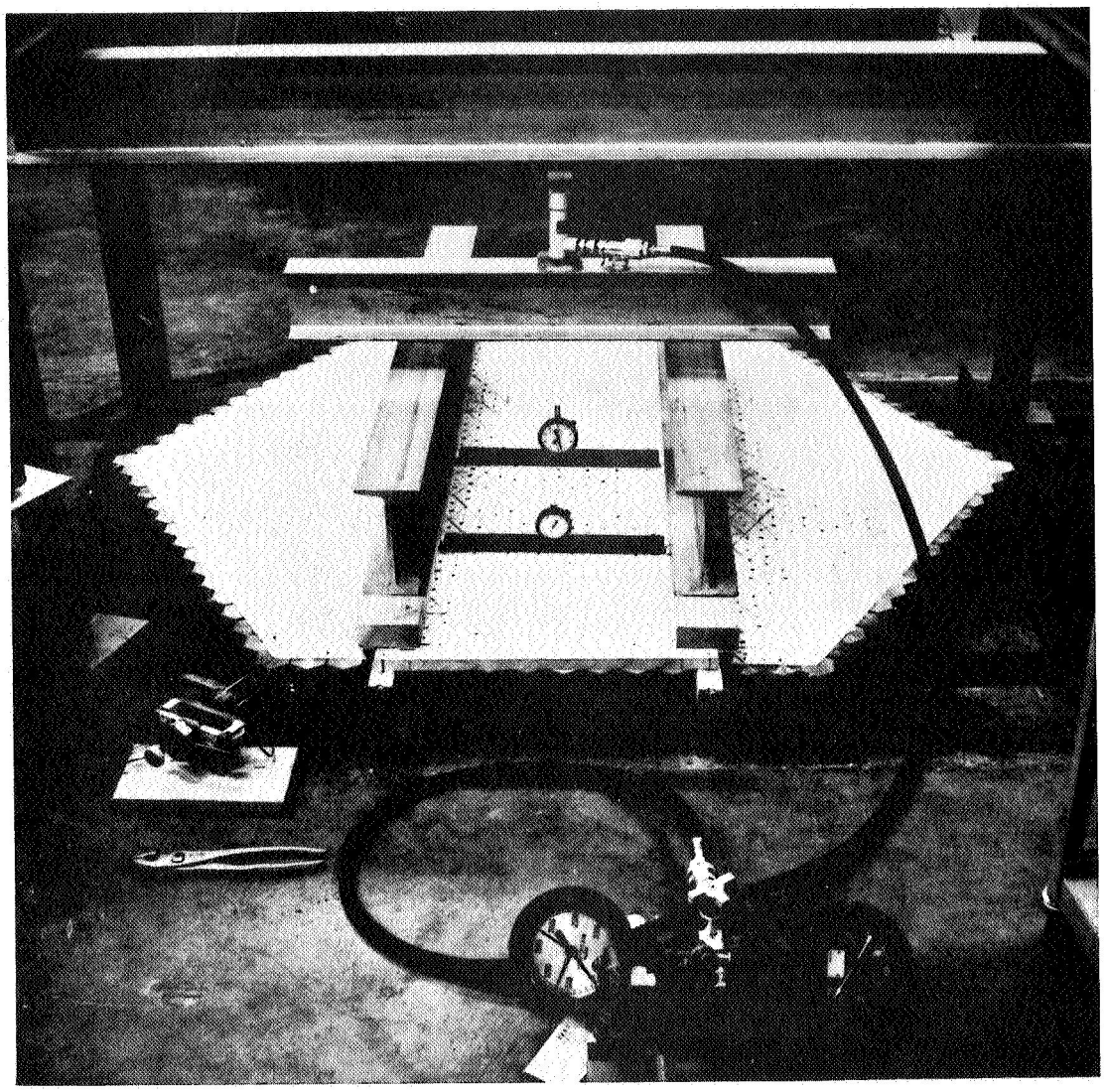

CYLINDRICAL BENDING TEST

Figure 9

$$M_{x_1} = \frac{8\frac{1}{2}}{53\frac{7}{16}} \quad \frac{P}{2}$$

$$= 0.0795 \text{ P (lb-in/in)}$$

and

$$M_{y_1} = \frac{13\frac{11}{16}}{48\frac{3}{16}} \quad \frac{P}{2}$$

$$= 0.1420 \text{ P (lb-in/in)}$$

Figure 7 shows M_{x_2} and M_{y_2} as

$$M_{x_2} = \frac{8\frac{1}{2}}{53\frac{11}{16}} \quad \frac{P}{2}$$

$$= 0.0791 \text{ P (lb-in/in)}$$

and

$$M_{y_2} = \frac{13\frac{13}{16}}{48\frac{1}{16}} \quad \frac{P}{2}$$

$$= 0.1437 \text{ P (lb-in/in)}$$

Figure 8 shows M_{x_3} and M_{y_3} as

$$M_{x_3} = \frac{8\frac{1}{2}}{53\frac{10}{16}} \quad \frac{P}{2}$$

$$= 0.0793 \text{ P (lb-in/in)}$$

and

$$M_{y_3} = \frac{13\frac{3}{4}}{48\frac{1}{8}} \frac{P}{2}$$

$$= 0.1429\ P\ (\text{lb-in/in})$$

The measurements of curvature between the ends of the curvature gage can be shown to be given by the following equation (See Appendix Equation A1)

$$1/R_{m_i} = \frac{2d}{L_i^2} = 0.0492\ d\ (\text{in}^{-1})$$ [17]

where $i = 1, 2, 3.$

$m = x.y.$

R_{m_i} = the radius of the ben plate

d = the deflection measurement

L_i = the distance between the gage probe and the stationary legs (L_i = 6.375 inches)

Ideally, the cylindrical bending test would be conducted so that the plate is bent to a cylindrical surface causing a curvature about one axis and allowing no curvature about the secondary axis. The test results showed that a secondary curvature occurred during the cylindrical bending tests. The bending moment about one axis is plotted against both primary and secondary curvatures which are shown in Figures 10 through 15. The graphs of the moment versus curvature (primary and secondary) are linear in each case. Each point of the curve was obtained from the average value of relative deflections over five points on the plate measured in two tests. The primary and secondary curvatures in each bending test are opposite in sign and the magnitude of secondary curvature is comparatively small. The secondary bending is due to the initial warpage of the plate after prestressing.

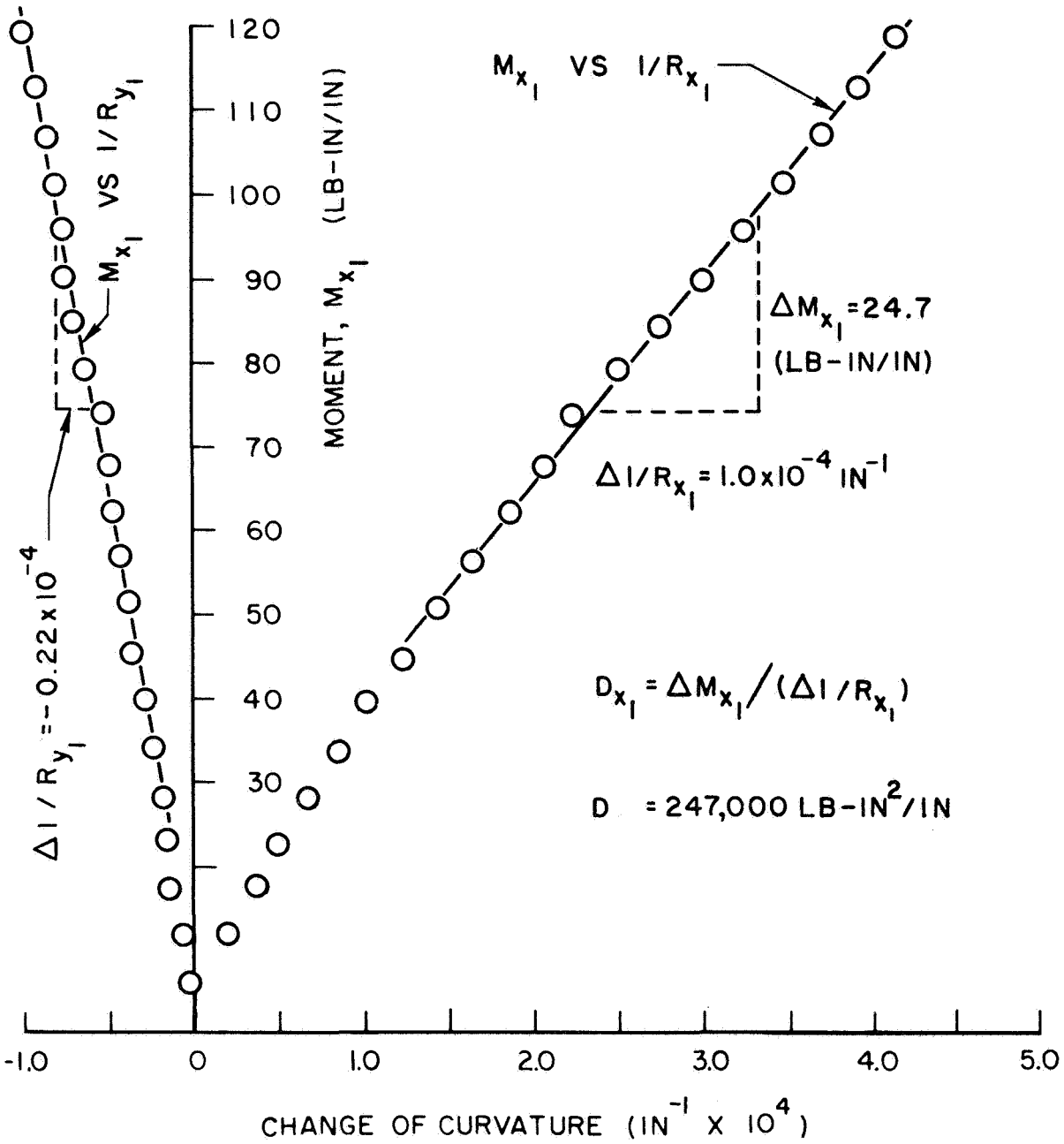

MOMENT VERSUS CURVATURE FOR CYLINDRICAL BENDING IN x_1–AXIS

Figure 10

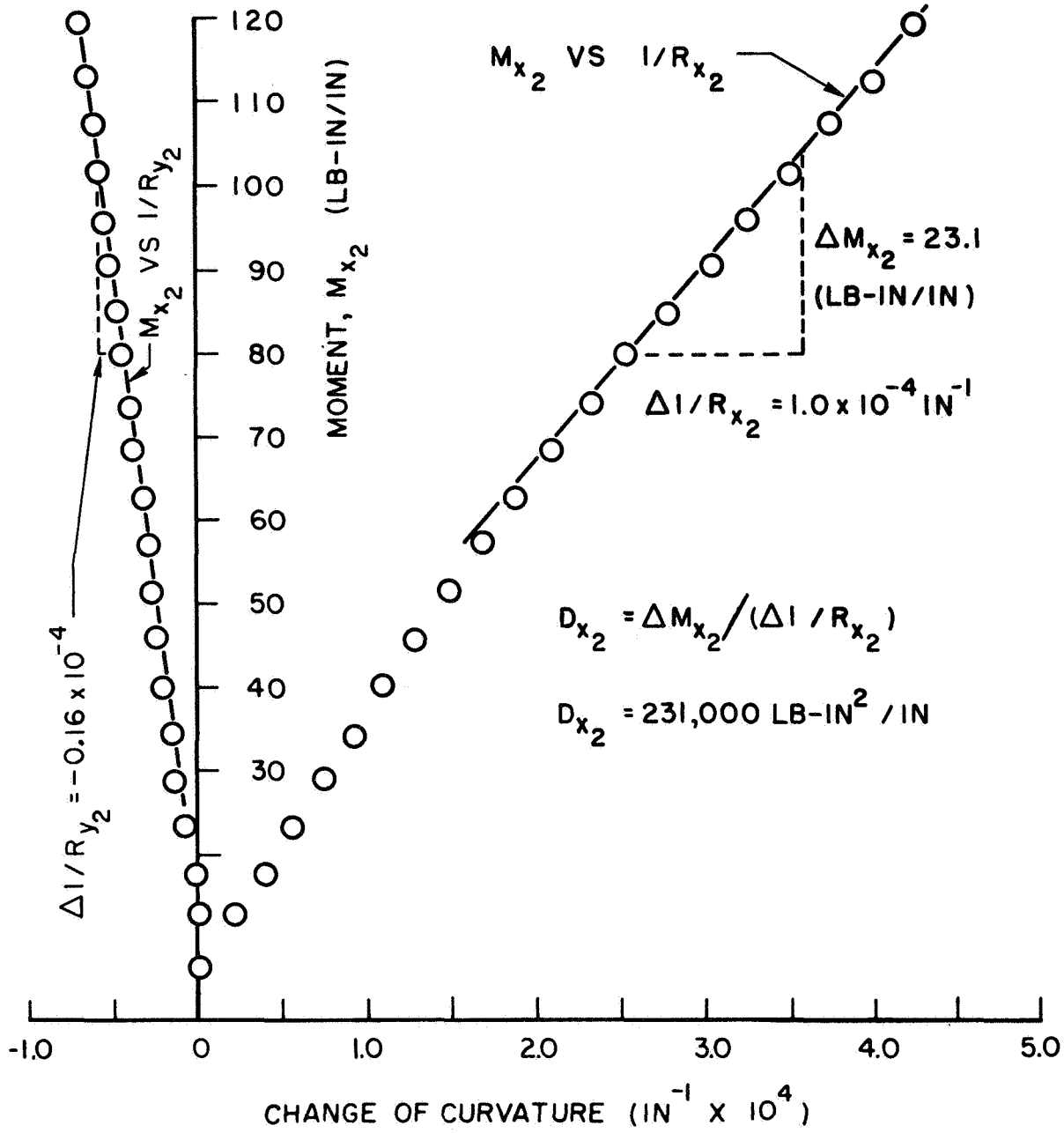

MOMENT VERSUS CURVATURE FOR CYLINDRICAL BENDING IN x_2–AXIS

Figure 11

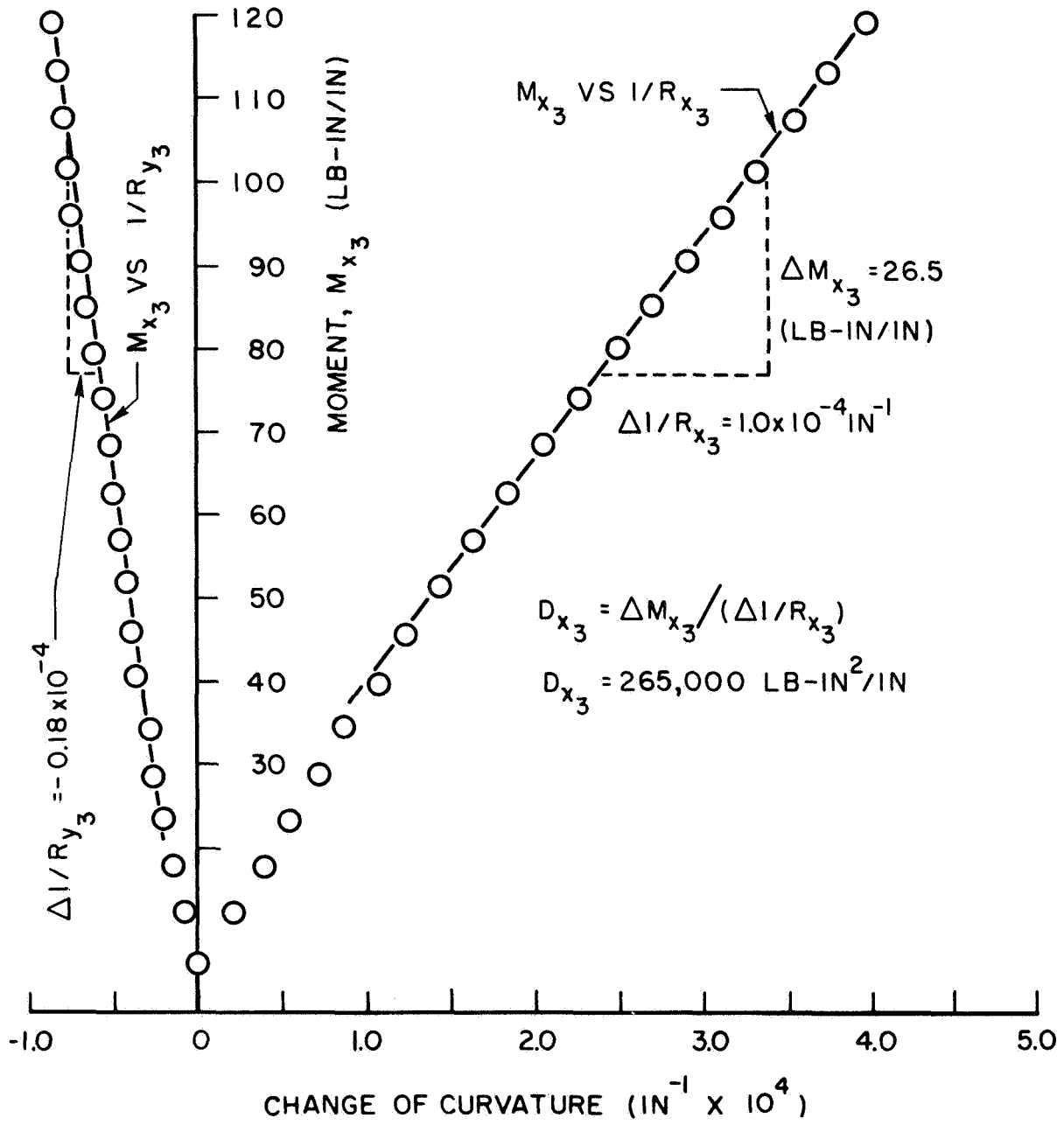

MOMENT VERSUS CURVATURE FOR CYLINDRICAL BENDING IN x_3–AXIS

Figure 12

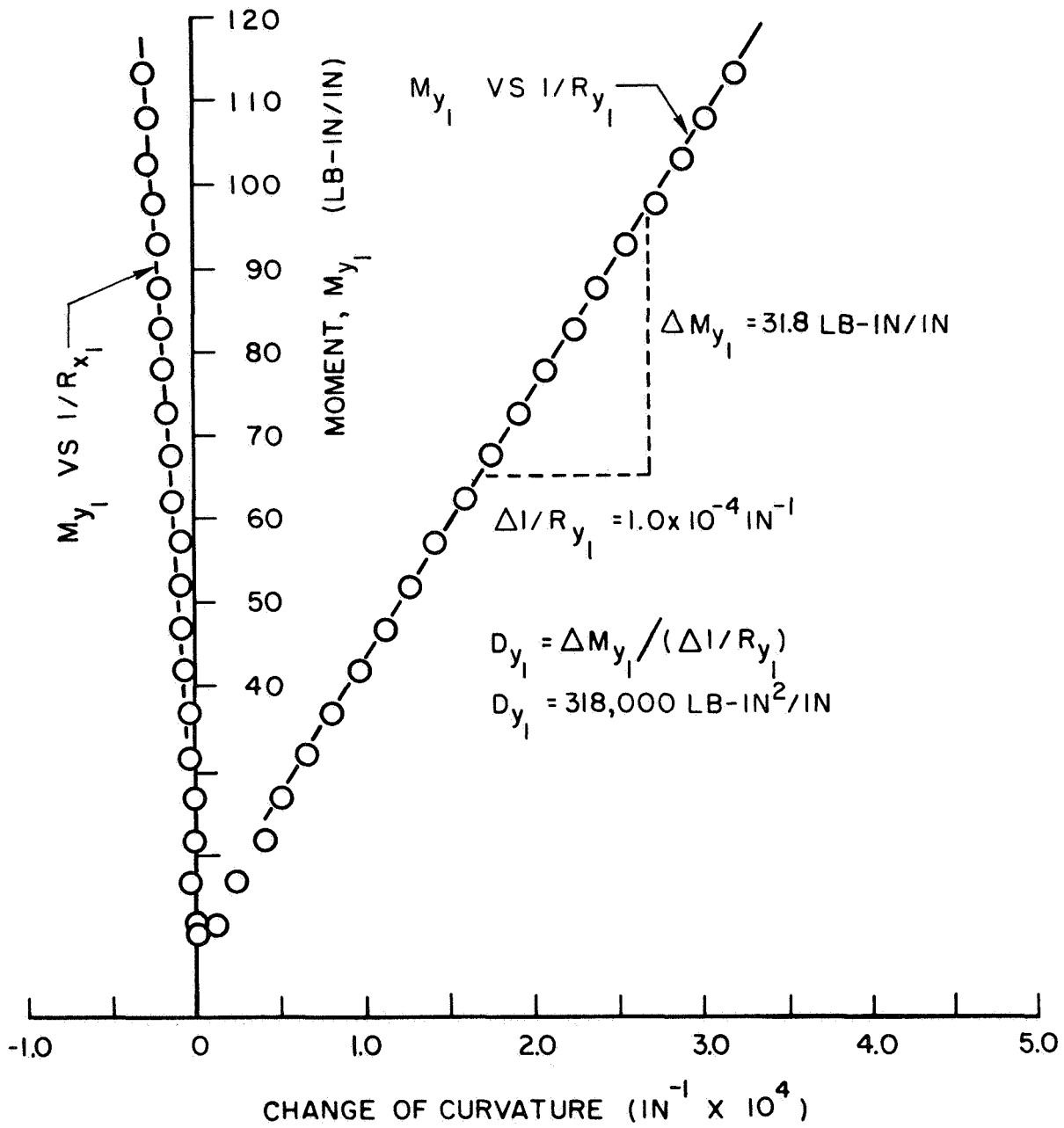

MOMENT VERSUS CURVATURE FOR CYLINDRICAL BENDING IN y_1–AXIS

Figure 13

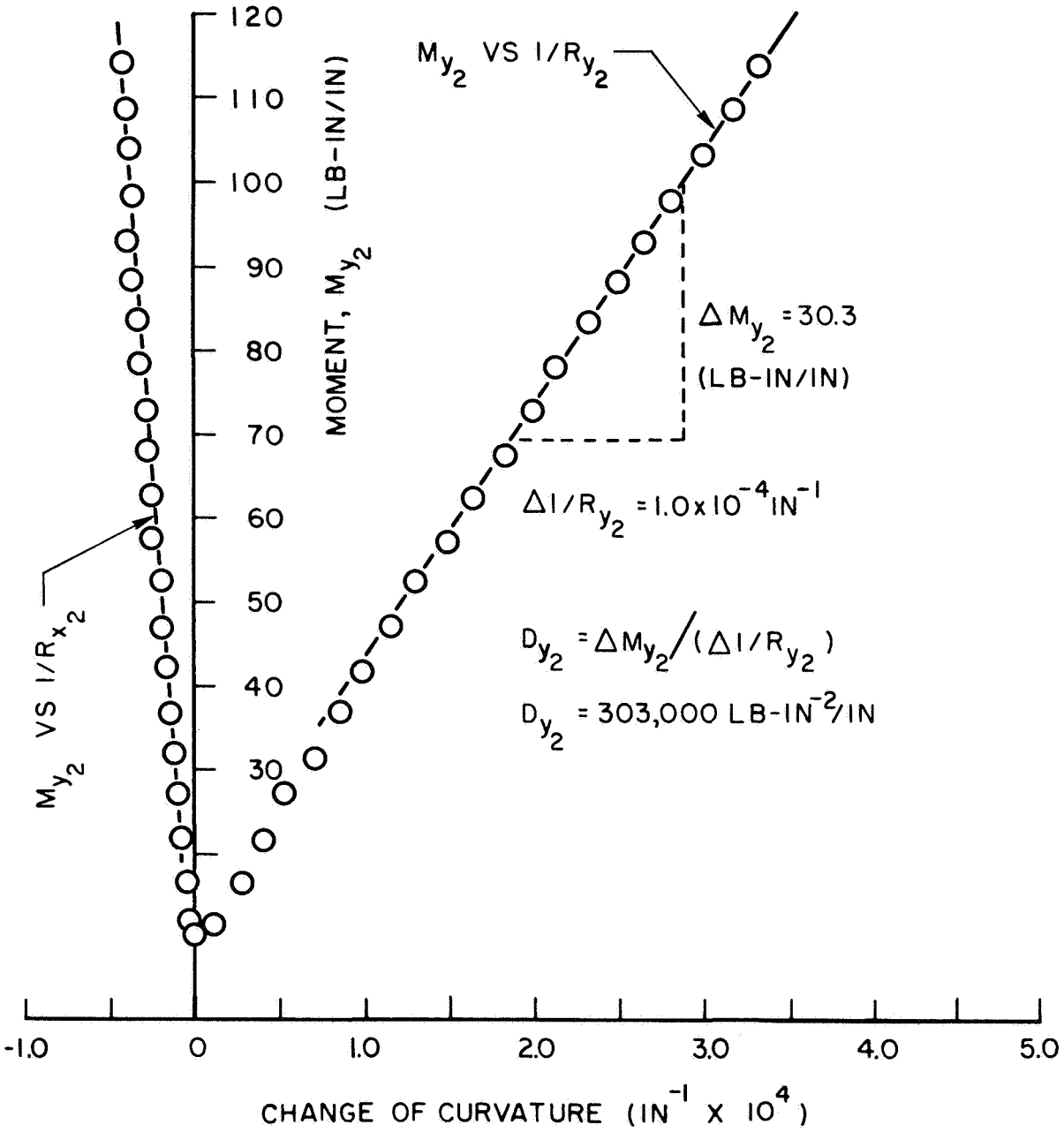

MOMENT VERSUS CURVATURE FOR CYLINDRICAL BENDING IN y_2–AXIS

Figure 14

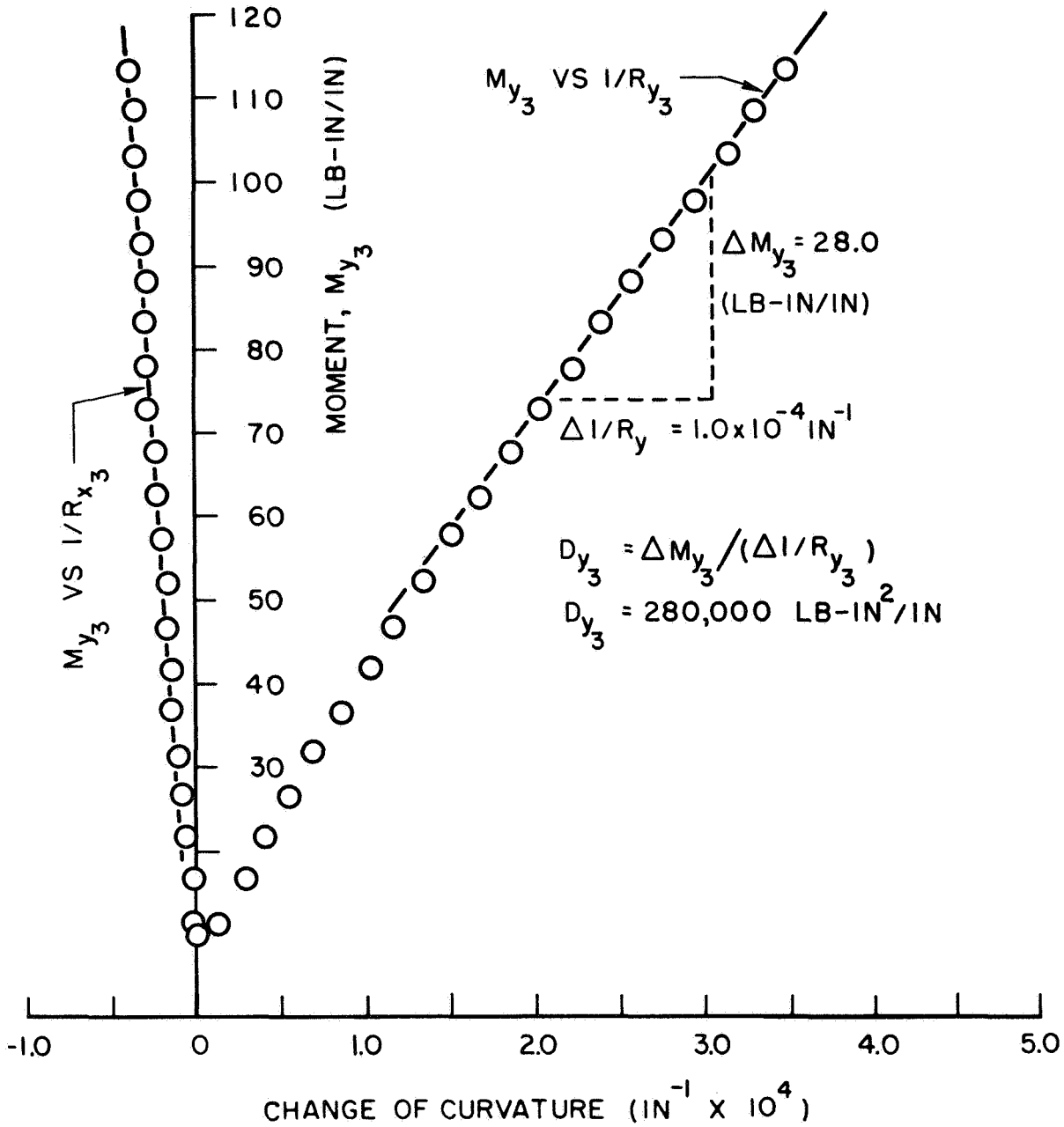

MOMENT VERSUS CURVATURE FOR CYLINDRICAL BENDING IN y_3–AXIS

Figure 15

The prestressing system is considered to be satisfactory since the relative deflections at five points in each case were reasonably uniform.

In Figures 10 through 15, the slope of the moment versus curvature plot is constant and is equal to the flexural rigidity constants D_{x_i} or D_{y_i} (Equations 7 and 8). The values of flexural rigidities in three sets of directions are given in the following table:

TABLE II

FLEXURAL RIGIDITIES

	D_{x_i}	D_{y_i}
1.	247,000 lb-in^2/in	318,000 lb-in^2/in
2.	231,000	303,000
3.	265,000	280,000

It is apparent from this table that D_{y_i} is consistently greater than D_{x_i} and the D_{y_i} are all of somewhat the same value while the D_{x_i} are all of a somewhat different value. This suggests that an appropriate analytical model of this plate must have properties such that the bending stiffness varies between a maximum and a minimum each 60°. No theoretical model with these properties is known.

(b) Twisting Test:

The plate was twisted by applying load to the corners of a 35-3/8 x 35-3/8 inch square parallel to the x, y, axes. Figure 16 is a photograph illustrating the twisting test. The force to twist the plate was developed by a two-ton hydraulic jack (same jack as in the bending tests) that pushed up at one corner of the plate while one pair of diagonally opposite corners were held down by two twenty-ton jacks used for positioning only. The fourth corner was held up with an aluminum half-round block which rested

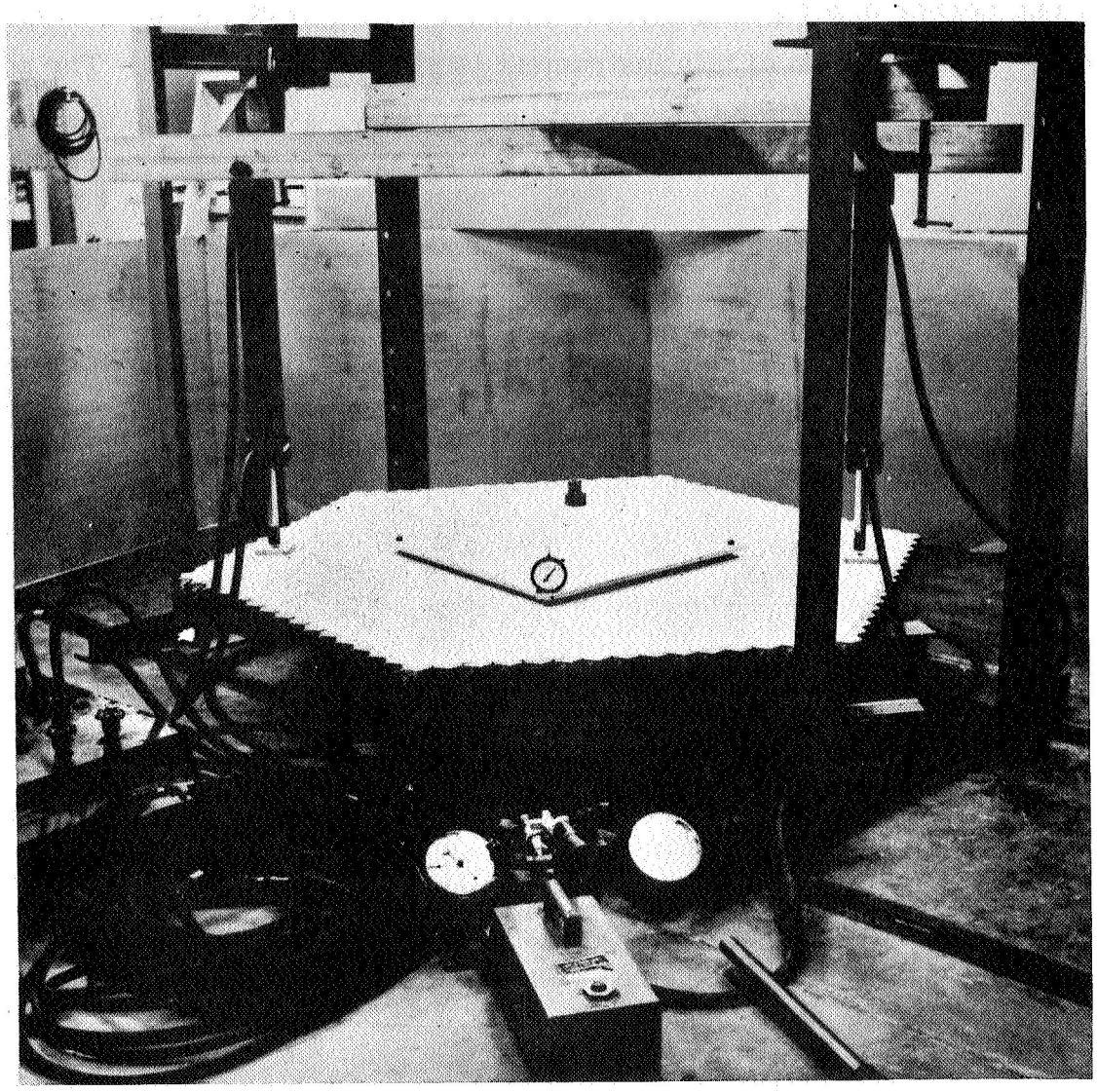

TWISTING TEST, FRONT VIEW

Figure 16

on the floor of the testing laboratory. The deflections of the twisted plate were measured by a twisting gage which consisted of a dial gage mounted at one corner of a square, 20" x 20" x 1/2", of plywood with three stationary legs. A description of this instrument is given in Appendix I. The plate was subsequently twisted about the x_2y_2 and x_3y_3 axes as indicated in Figure 17.

The theory given by Timoshenko[5] shows that concentrated loads P at each corner produce a twisting moment $M_{x_iy_i}$ per unit length along each side equal to P/2. The relation between the curvature and the twisting plate deflection, read directly from twist gage, can be given by the following equation (see Appendix, Equation A2)

$$1/R_{x_iy_i} = \frac{\delta_{x_iy_i}}{L^2_{x_iy_i}} \tag{20}$$

where $i = 1, 2, 3$.

$R_{x_iy_i}$ = the radius of the twisting plate

$\delta_{x_iy_i}$ = the deflection measurement

$L_{x_iy_i}$ = length of square twist gage ($L_{x_iy_i}$ = 20 inches)

So that

$$1/R_{x_iy_i} = \frac{\delta_{x_iy_i}}{400} \quad \text{in}^{-1}$$

For the twisting tests, the average deflection, $\delta_{x_iy_i}$, is plotted against the magnitude of the load $P_{x_iy_i}$ in Figures 18, 19, and 20. Five tests were conducted in each case and the observed values of deflection repeated satisfactorily. At low values of upward force, before the pair of diagonally downward forces acted on the plate, the plate deflected slightly due to its

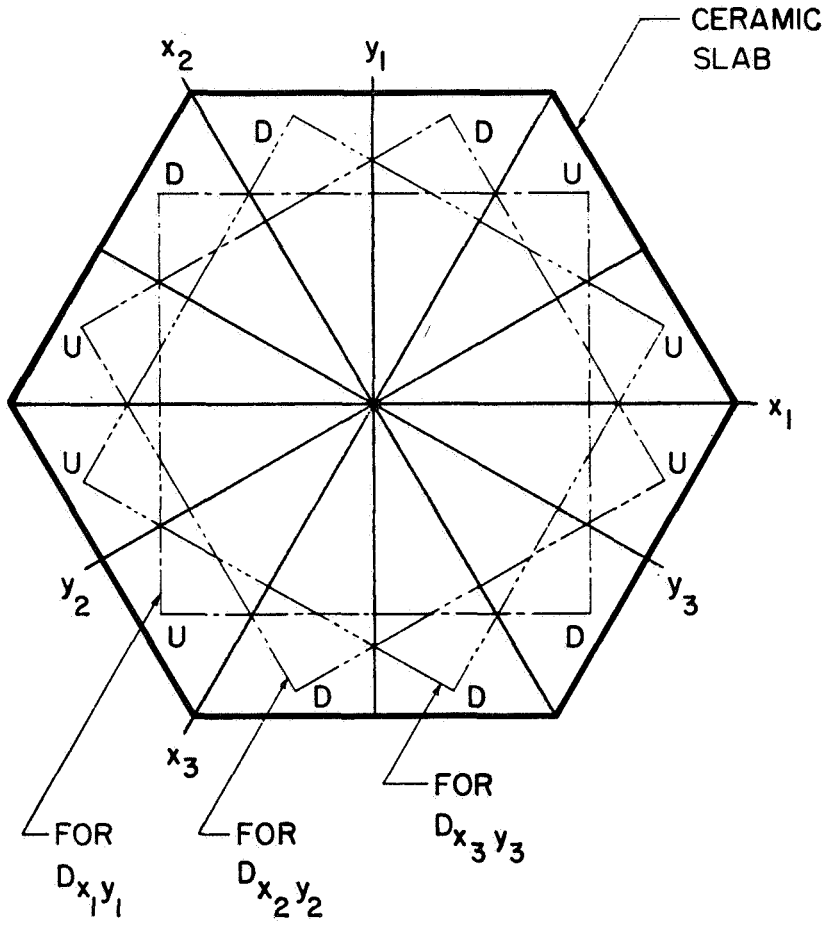

U = UPWARD FORCE
D = DOWNWARD FORCE

LAYOUT OF THREE SQUARES (35-3/8" x 35-3/8") ON THE SLAB FOR TWISTING TESTS

Figure 17

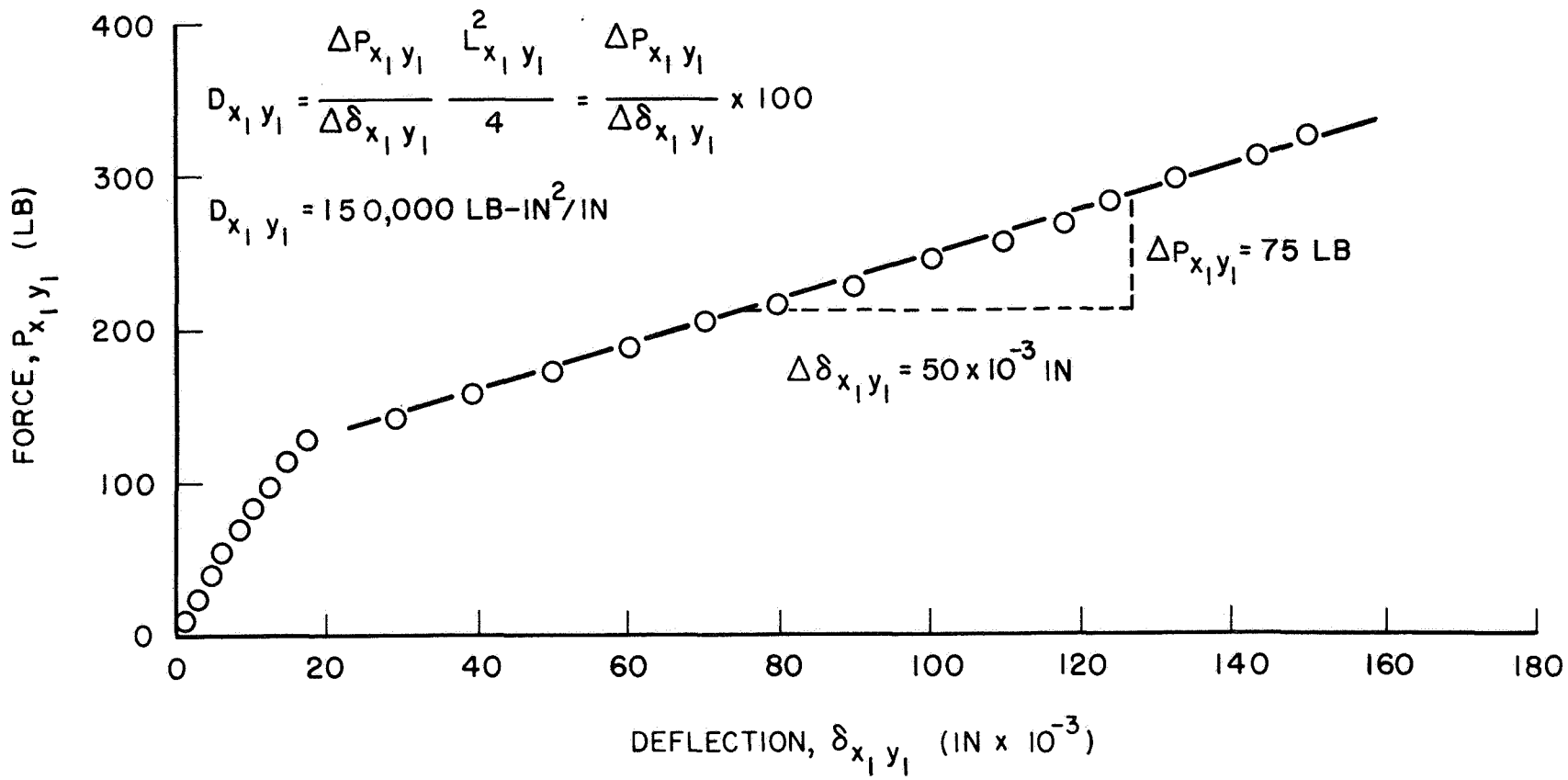

FORCE VERSUS DEFLECTION OF TWISTING TEST FOR $D_{x_1 y_1}$

Figure 18

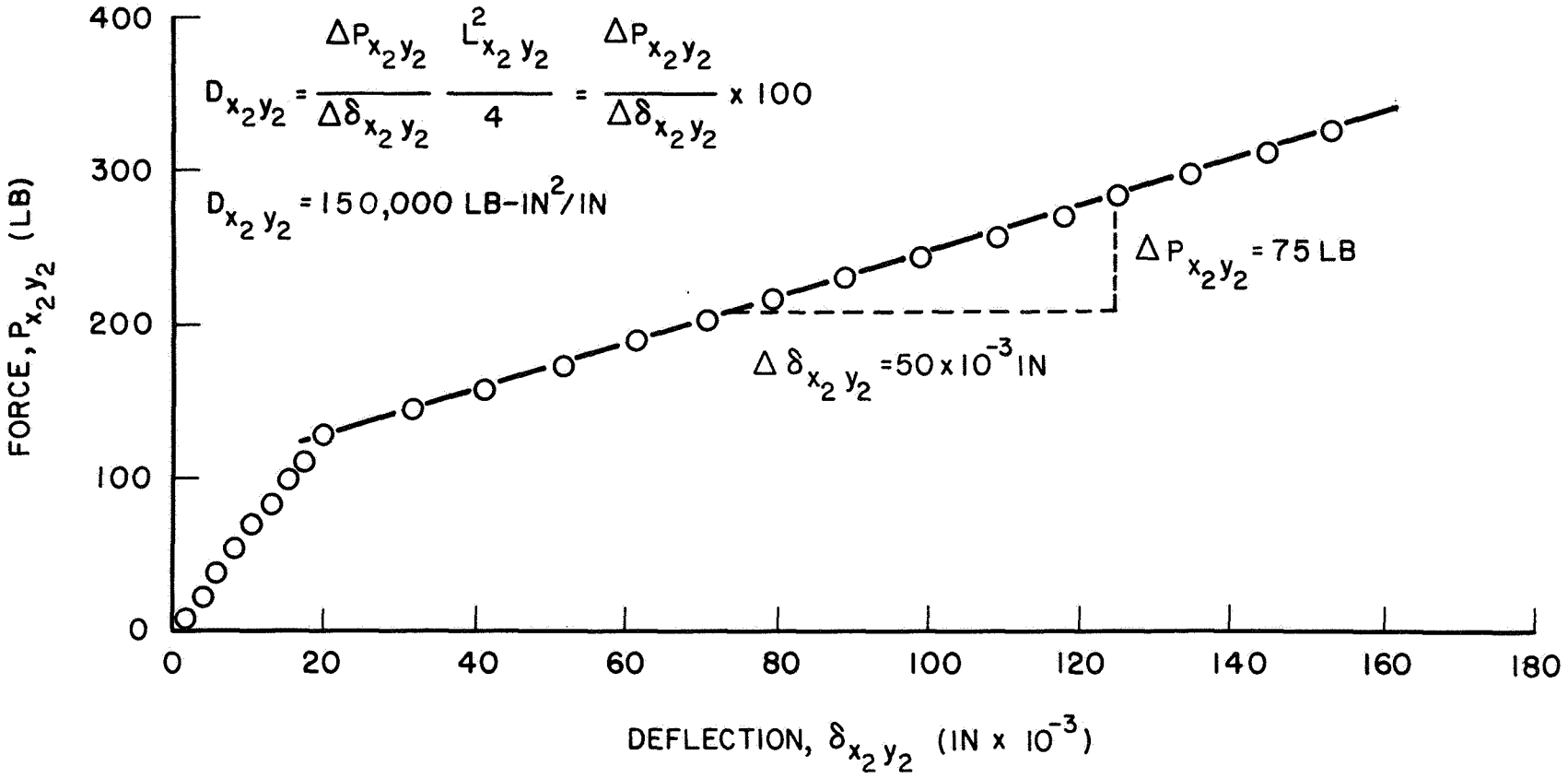

FORCE VERSUS DEFLECTION OF TWISTING TEST FOR $D_{x_2y_2}$

Figure 19

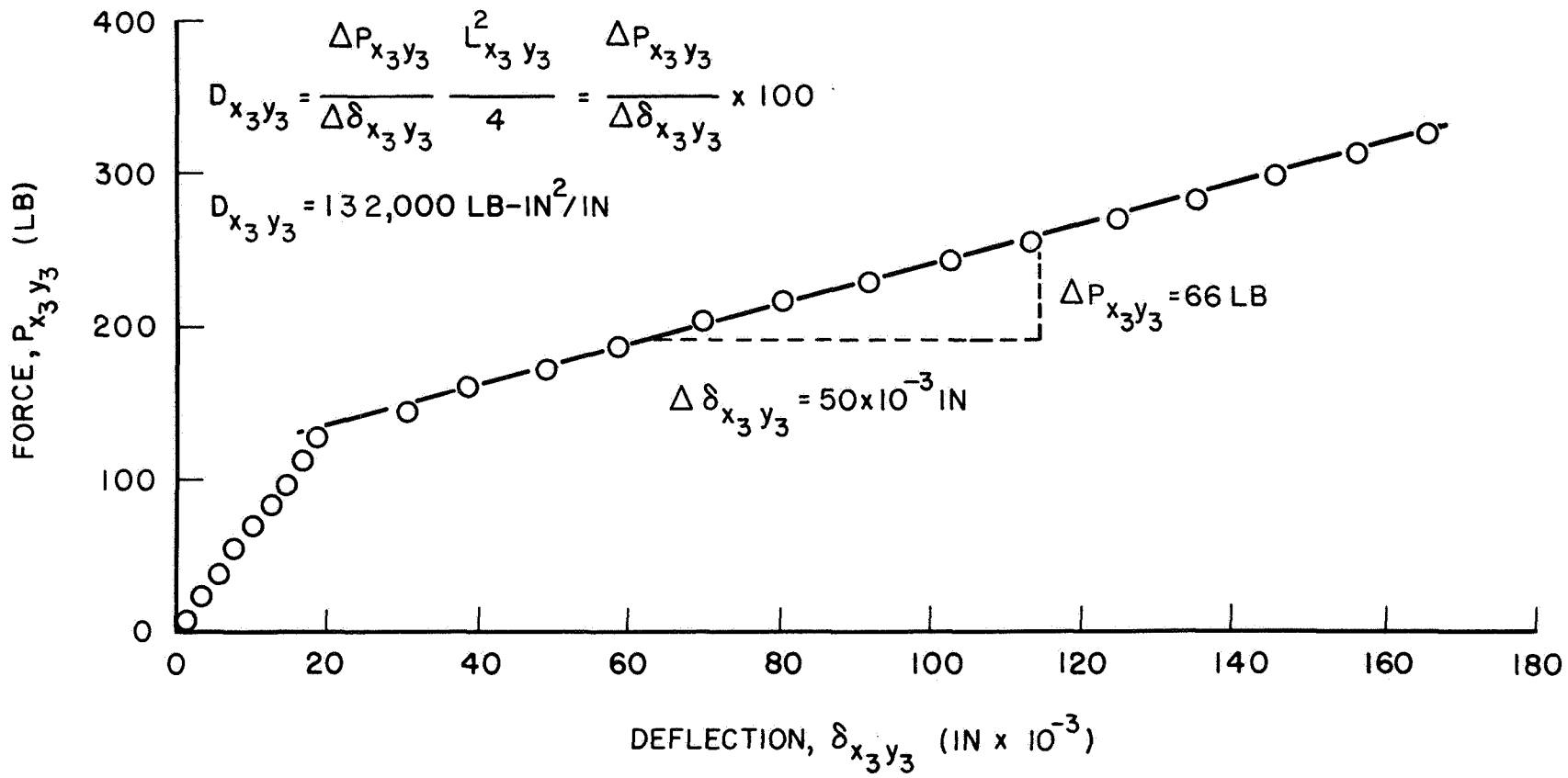

FORCE VERSUS DEFLECTION OF TWISTING TEST FOR $D_{x_3y_3}$

Figure 20

dead load. At high values of twisting force, the $P_{x_iy_i}$ versus $\delta_{x_iy_i}$ were relatively linear. The twisting rigidity $D_{x_iy_i}$ is the slope of $P_{x_iy_i}$ versus $\delta_{x_iy_i}$ curve multiplied by constant, as shown by Equation (A3) in the Appendix. The values of twisting rigidity in three directions are given in the following table:

TABLE III

TWISTING RIGIDITIES

$D_{x_1y_1}$	150,000 lb-in^2/in
$D_{x_2y_2}$	150,000
$D_{x_3y_3}$	132,000

In comparing the magnitudes given in Table III with those in Table II, the twisting rigidities $D_{x_iy_i}$ are smaller than the flexural rigidities D_{x_i} of D_{y_i} and are about half the magnitudes of flexural rigidities. According to the theory of anisotropic plates, on Page 365 of Reference 5, the ratio of D_{xy} and D_y can be written as

$$\frac{D_{xy}}{D_y} = \frac{G}{E'_y} \qquad \text{since} \qquad D_{xy} = \frac{Gh^3}{12}$$

$$D_y = \frac{E'h^3}{12}$$

In the particular case of isotropy we have

$$E'_y = \frac{E}{1-\nu^2}$$

$$G = \frac{E}{2(1+\nu)}$$

then

$$\frac{D_{xy}}{D} = \frac{1}{2}(1-\nu) \tag{22}$$

If we assume that $\nu = \frac{1}{5}$ (see Table I) (23)

thus

$$\frac{D_{xy}}{D_y} = \frac{1}{2}\left(1 - \frac{1}{5}\right) = \frac{2}{5} \tag{24}$$

Our results show that, for the case of the prestressed plate,

$$\frac{D_{x_i y_i}}{D_{y_i}} = \frac{1}{2} \tag{25}$$

Therefore, the ratios of twisting rigidities and flexural rigidities of the experimental results are reasonable.

(c) Anticlastic Bending Tests:

A whippletree fixture was fabricated to study the anticlastic bending behavior. The fixture is so designed that the plate can be bent in a primary direction while bending freely in a secondary direction due to the Poisson effect. Figure 21 shows the whippletree fixture in use. The ceramic plate was attached to the whippletree fixture by high strength 1/32-inch diameter steel wires. The ends of the wire were silver soldered to 1/8-inch diameter steel bolts, one end attached to the whipple tree fixture and the other end passed through a hole pre-drilled in the plate where it was fixed by nuts. Two fixtures were suspended from the ceiling of the laboratory and the other two fixtures were simultaneously attached to an ARA testing machine.*

The anticlastic bending tests were conducted in three y_i directions by applying the moment M_{y_i} only. As $M_{x_i} = 0$, Equation (11) gives:

$$D_{I_i} = - D_{x_i} \frac{1/R_i}{1/R_{y_i}} = - D_{x_i} \nu_i \tag{11}$$

*Allied Research Associates, Model PD4-18 Universal Testing Machine.

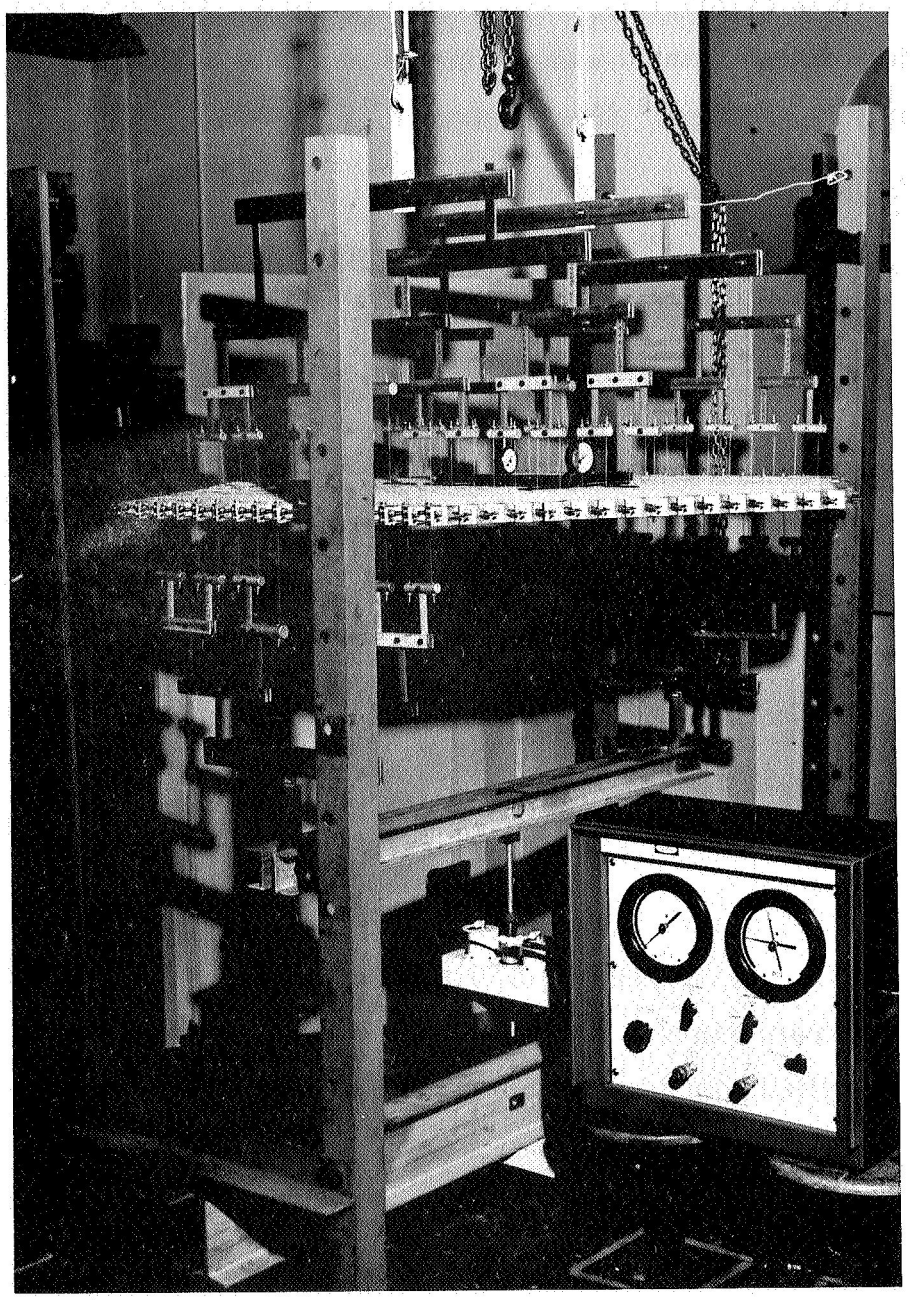

ANTICLASTIC BENDING TEST

Figure 21

The plate curvatures were measured by a curvature gage which was introduced in cylindrical bending tests. The positions of loading and curvature measurement were same as shown in cylindrical bending tests in y_i directions. (See Figures 6, 7, and 8.)

When the bending moment M_{y_i} (i = 1, 2, 3) was applied to the plate, the whippletree fixture permitted the plate to bend with a primary curvature $1/R_{y_i}$ and a secondary curvature $1/R_{x_i}$ due to the Poisson effect. The applied moment M_{y_i} is plotted against both $1/R_{y_i}$ and $1/R_{x_i}$ in Figures 22, 23 and 24. The dead load of 34 pounds due to weight of the fixture and the loading systems has been added into calculation. Each point on the curves is obtained from the average value of six observed relative deflections which were determined at three points (A, 0, and B as shown in Figures 6, 7, and 8) on the plate in two separate tests. The data from points C and D are not used in calculation, since the locations at C and D are outside of the effective loading area, the curvature measurements at C and D are slightly lower than those of other three points.

The flexural rigidities in three y_i directions from the anticlastical bending tests are 310,000 lb-in^2/in, 295,000 lb-in^2/in, and 280,000 lb-in^2/in (from Figures 22, 23 and 24) which are consistent with those from the cylindrical bending test in the y_i directions.

The Poisson rigidity constants are calculated from Equation (11), where D_{x_i} in each direction is from cylindrical bending tests. The values are given in Table II. The Poisson Ratio is obtained from the ratio of secondary curvature to primary curvature. The Poisson ratios and the Poisson rigidities in three directions are given in the following table:

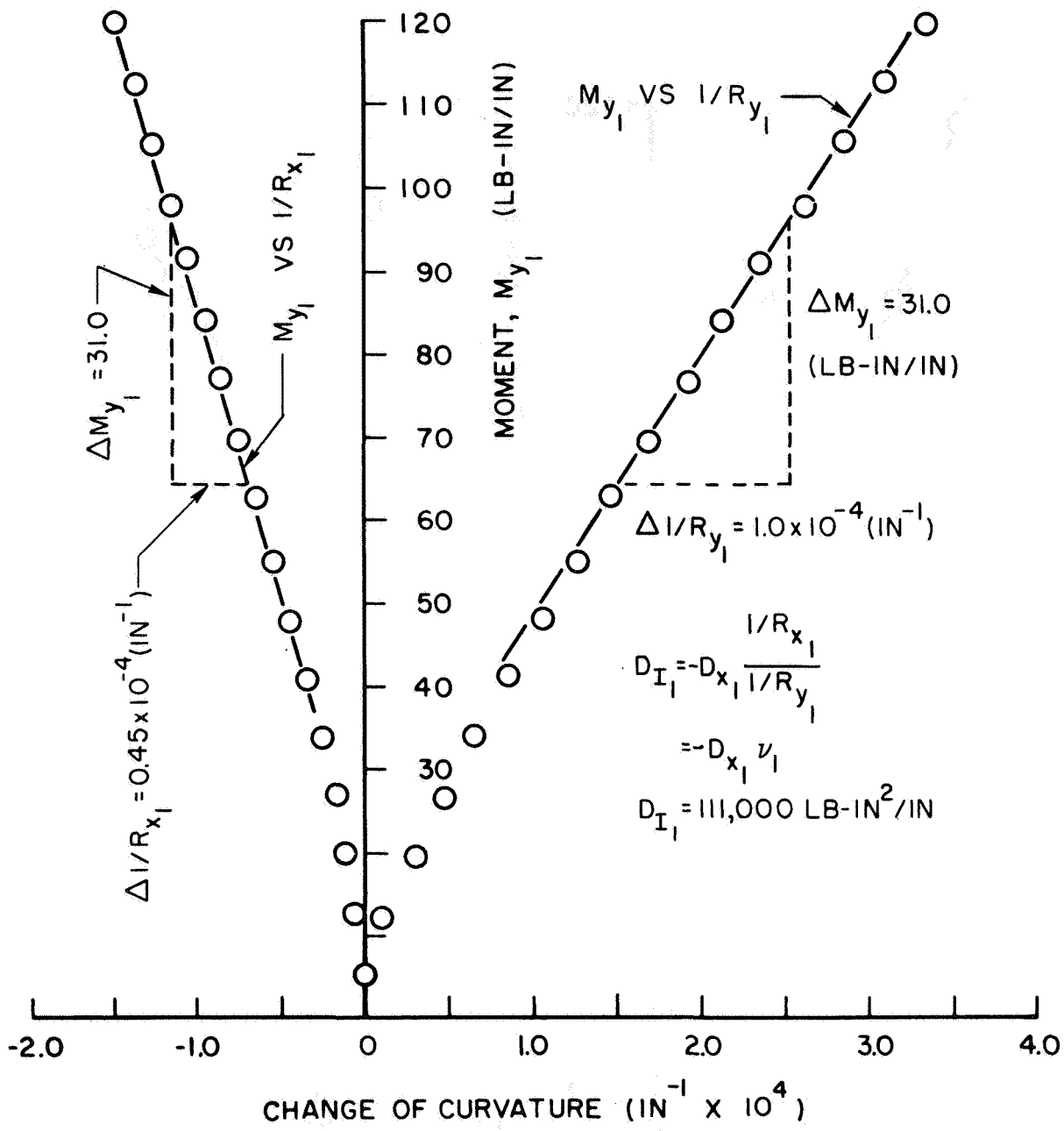

MOMENT VERSUS CURVATURE FOR ANTICLASTIC BENDING IN y_1–DIRECTION

Figure 22

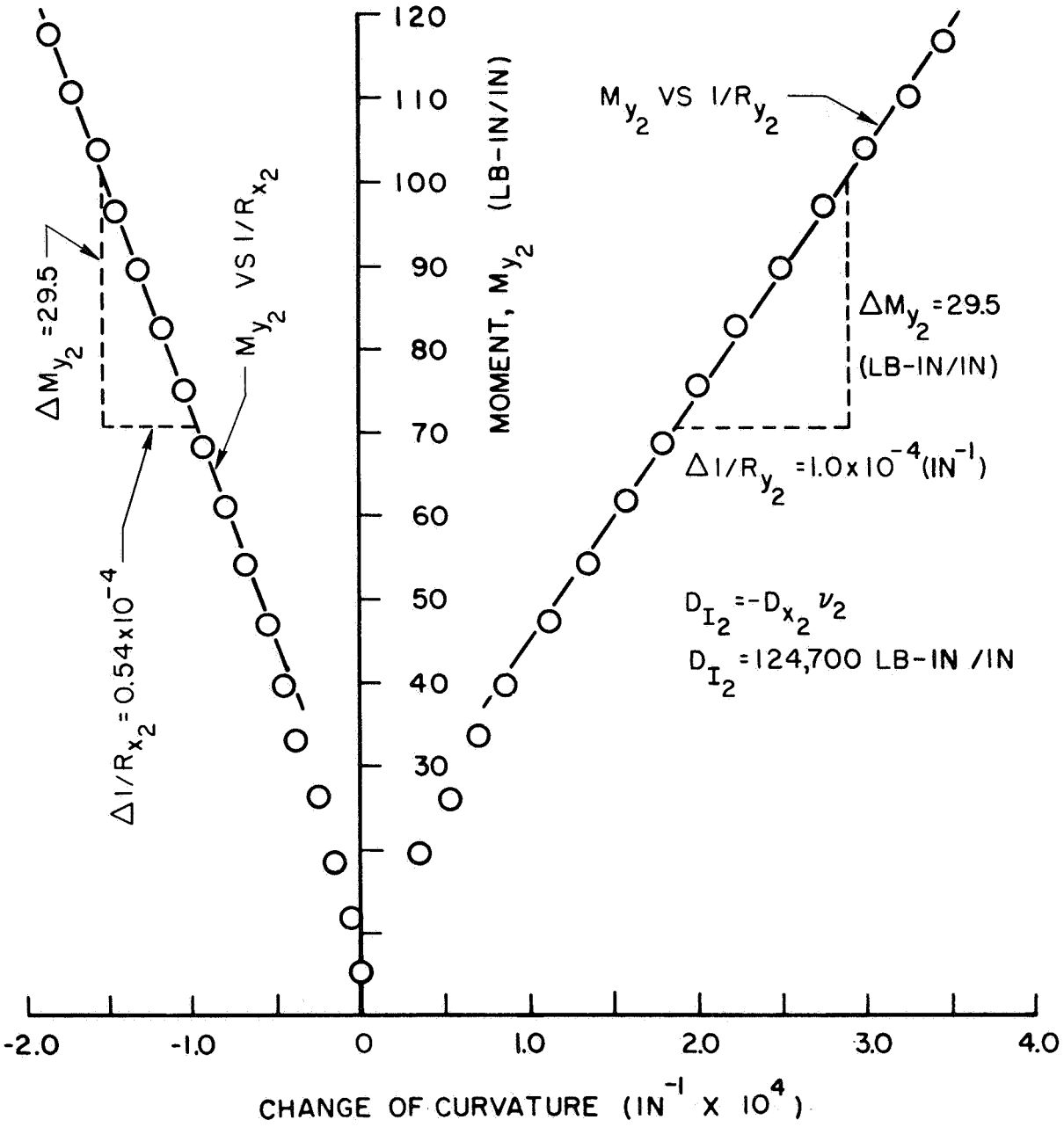

MOMENT VERSUS CURVATURE FOR ANTICLASTIC BENDING IN y_2–DIRECTION

Figure 23

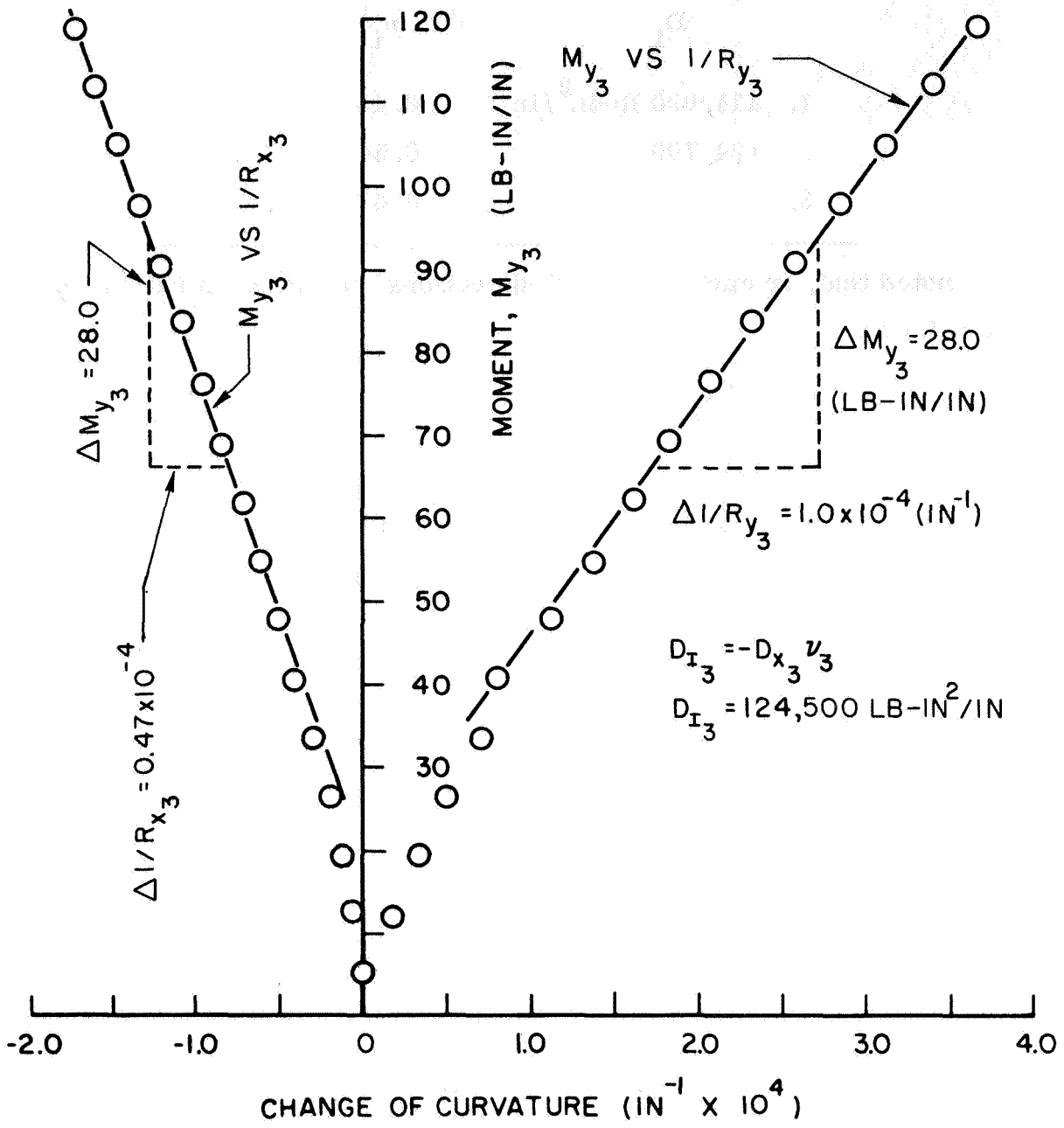

MOMENT VERSUS CURVATURE FOR ANTICLASTIC BENDING IN y_3–DIRECTION

Figure 24

TABLE IV

POISSON RIGIDITIES AND POISSON RATIOS

	D_{I_i}	ν_i
1.	111,000 lb-in^2/in	0.45
2.	124,700	0.54
3.	124,500	0.47

It is noted that, in each set of $x_i y_i$ directions, the Poisson ratio ν_i here has the relation:

$$\nu_i = \sqrt{\nu_{x_i} \nu_{y_i}} \tag{26}$$

The excessively high values of Poisson ratio in Table IV are an indication of the inadequacy of orthotropic plate theory for describing the behavior of this plate.

IV SUMMARY AND CONCLUSIONS

In this investigation the rigidity properties of a three-way prestressed segmented ceramic plate were studied experimentally. The studies made and the quantities determined for the plate were based upon the fact that the plate was considered to be orthotropic in three sets of orthogonal axes. The plate prestress is seen to be satisfactorily uniform since the rigidities did not significantly depend on the measurement locations or directions. A few segments of the ceramic material cracked because of compressive stress concentrations, but the plate retained its load bearing capacity. The experimental determination of the plate rigidities in three directions are listed in the following table

TABLE V

PLATE RIGIDITIES (lb-in^2/in) AND POISSON'S RATIO

	D_{x_i}	D_{y_i}	$D_{x_i y_i}$	D_{I_i}	ν_i
1.	247,000	318,000	150,000	111,000	0.45
2.	231,000	303,000	150,000	124,700	0.54
3.	265,000	280,000	132,000	124,500	0.47

These results are reasonably constant for the 1, 2, and 3 directions and imply that there are three sets of "principal" axes in the plane.

The twisting rigidities $D_{x_i y_i}$ are about half of the magnitude of flexural rigidities D_{x_i} and D_{y_i}. This is verified to be reasonable in comparison with an isotropic plate. However, if we substitute the value of $\nu_i = \frac{1}{2}$ (from Table V) into Equation (23), we obtain

$$\frac{D_{x_i y_i}}{D_{y_i}} = \frac{1}{4}$$

Obviously, this result is inconsistent. The value of Poisson ratio in the three directions is excessively high.

BIBLIOGRAPHY

1. Johnston, R. D., R. D. Chipman and W. J. Knapp, "Prestressed Ceramics as a Structural Material," J. Am. Cer. Soc., 36, No. 4, pp. 121-126, 1953.

2. Nikolaychik, G., R. B. Matthiesen, and W. J. Knapp, "Bending-Stiffness Properties of a Prestressed Segmented Ceramic Plate," NASA Contractor Report, UCLA Report No. 65-26, June 1965.

3. Weiss, D., P. Kurtz and W. J. Knapp, "Strength of Specimens Containing Parallel Cylindrical Holes," Am. Cer. Soc. Bull., Vol. 45, No. 8, pp. 695-697, August 1966.

4. Huber, M. T., "Die Grundlagen Einer Rationellen Berchnung der Kreuzweise bewehrten Eisenbetonplatten," Z. des Osterr Ing. und Arch. Ver. No. 30, pp. 557-564, 1914.

5. Timoshenko, S. and S. Woinowsky-Krieger, Theory of Plates and Shells, 2nd ed. New York, McGraw-Hill, pp. 42-46, 364-369, 1959.

6. Lekhnitskii, S. G., Theory of Elasticity of an Anisotropic Elastic Body, Translated by P. Fern, San Francisco, Holden-Day, Inc., pp. 1-32, 1963.

7. Hearmon, R. F. S., E. H. Adams, "The Bending and Twisting of Anisotropic Plates," British J. of App. Physics, Vol. 3, pp. 150-156, 1952.

8. Huffington, N. J. Jr., "Theoretical Determination of Rigidity Properties of Orthogonally Stiffened Plates," J. of App. Mech., Vol. 23, pp. 15-20, March 1956.

9. Kingery, W. D., Introduction to Ceramics, 2nd Printing, New York, Wiley, pp. 51-56, June 1963.

APPENDIX

(1) Curvature Gage

The plate curvature was measured by a curvature gage. A photograph of this instrument is given on Figure 9. A dial gage, reading directly to 10^{-4} inches, was mounted on a steel bar halfway between two stationary legs. The two stationary legs and the probe of the gage made contact with the ceramic plate. When the plate was bent, the gage measured relative deflection between the middle and the end of the steel bar. Figure A1 gives a diagram of the curvature instrument resting against the bent plate. The following derivation of relative deflection "d" to plate curvature $1/R_m$. In Figure A1 the triangle OQS gives the relation as

$$R_m^2 = L^2 + \left(R_m - d\right)^2$$

where

R_m = the radius of the bent plate

d = the deflection measurement

L = the distance between the gage probe and the stationary leg $\left(L = 6\,\frac{24}{64}\text{ in}\right)$

Solving for R_m from the above equation, we have

$$R_m = \frac{L^2 + d^2}{2d}$$

or

$$1/R_m = \frac{2d}{L^2 + d^2}$$

Since L^2 is much greater than d^2, the latter can be neglected, so

$$1/R_m = \frac{2d}{L^2}$$

or

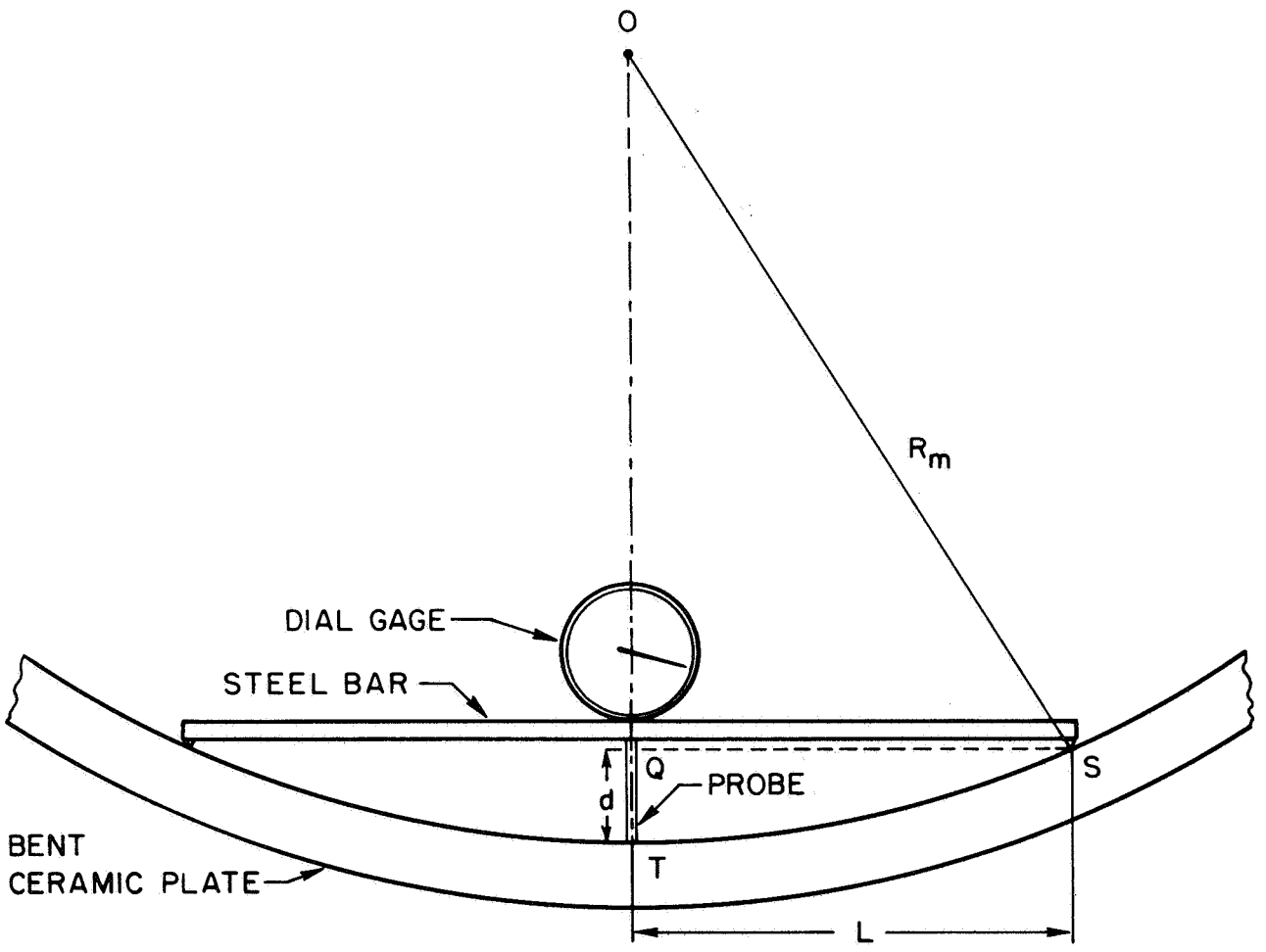

CURVATURE GAGE AND BENT PLATE

Figure A1

$$1/R_m = 0.0492\ d\ (in^{-1})$$

(2) Twist Gage

The twist of the plate was measured by a twist gage. A photograph of this instrument is given on Figure 11. A dial gage was mounted at one corner of a square of plywood with three stationary legs. When the plate was twisted, the gage measured the relative twisting deflection (δ_{xy}) from the difference of the gage probe and the stationary legs. If the length of the square twisting gage is L_{xy}, the diagonal distance of the legs is $\sqrt{2}\ L_{xy}$ Figure A2 gives the relation between the deflection δ_{xy} and the plate radius R_{xy} as following

$$R_{xy}^2 = \left(R_{xy} - \delta_{xy}\right)^2 + \left(\sqrt{2}\ L_{xy}\right)^2$$

Solving for $R_{x_i y_i}$ from this equation, we have

$$R_{xy} = \frac{\delta_{xy} + 2L_{xy}^2}{2\delta_{xy}}$$

or

$$1/R_{xy} = \frac{2\delta_{xy}}{\delta_{xy}^2 + 2L_{xy}^2}$$

Since L_{xy}^2 is much greater than δ_{xy}^2, the latter can be neglected, so

$$1/R_{xy} = \frac{\delta_{xy}}{L_{xy}^2}$$

Since L_{xy} = 20 inches, we have

$$1/R_{xy} = \frac{\delta_{xy}}{400}\ \ (in^{-1})$$

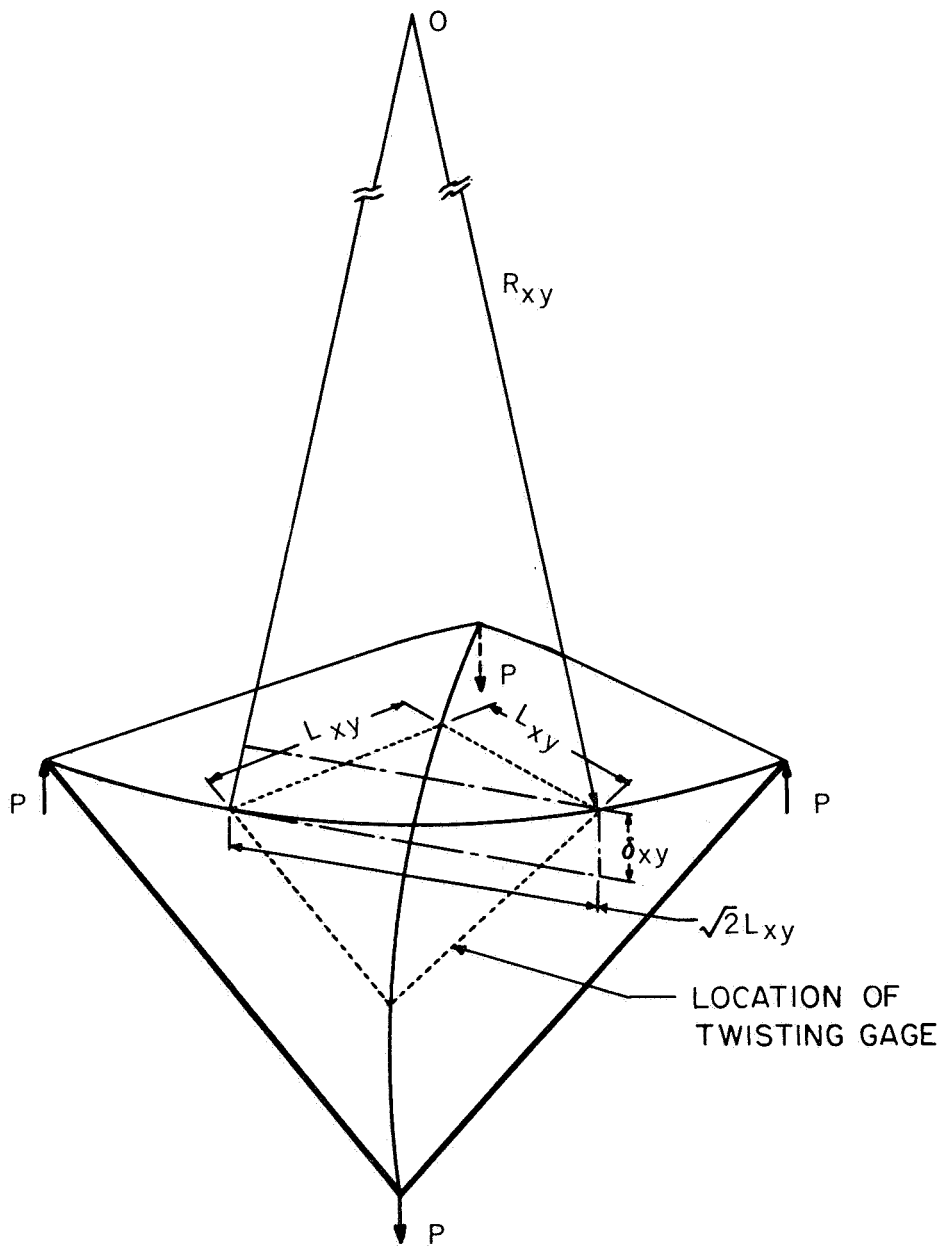

PLATE UNDER TWISTING MOMENT

Figure A2

when the twisting moment is

$$M_{xy} = \frac{1}{2} P$$

From Equation (10), the twisting rigidity is obtained as

$$D_{xy} = \frac{P}{\delta_{xy}} \times 10^2 \text{ lb-in}^2/\text{in}$$